AD-A119 758 AIR FORCE INST OF TECH WRIGHT-PATTERSON AFB OH F/G 4/1
THE MASS AND ANGULAR MOMENTUM BALANCE OF THE ZONALLY-AVERAGED G--ETC(U)
1981 R D TOWNSEND, D R JOHNSON
UNCLASSIFIED AFIT/CI/NR-81-34T NL

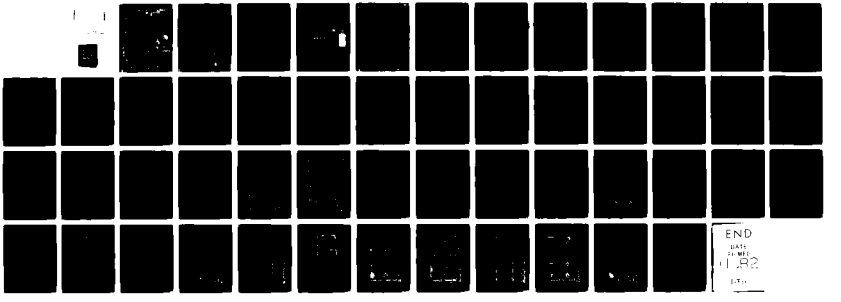

UNCLASS

SECURITY CLASSIFICATION OF THIS PAGE (When Data Entered)

REPORT DOCUMENTATION PAGE	READ INSTRUCTIONS BEFORE COMPLETING FORM
1. REPORT NUMBER AFIT/CI/NR-81-34T	2. GOVT ACCESSION NO. AD-A119758
3. RECIPIENT'S CATALOG NUMBER	
4. TITLE (and Subtitle) The Mass and Angular Momentum Balance of the Zonally-Averaged Global Circulation	5. TYPE OF REPORT & PERIOD COVERED THESIS/DISSERTATION
	6. PERFORMING ORG. REPORT NUMBER
7. AUTHOR(s) Ronald D. Townsend and Donald R. Johnson	8. CONTRACT OR GRANT NUMBER(s)
9. PERFORMING ORGANIZATION NAME AND ADDRESS AFIT STUDENT AT: Univ of Wisconsin-Madison	10. PROGRAM ELEMENT, PROJECT, TASK AREA & WORK UNIT NUMBERS
11. CONTROLLING OFFICE NAME AND ADDRESS AFIT/NR WPAFB OH 45433	12. REPORT DATE ? 1981
	13. NUMBER OF PAGES 26
14. MONITORING AGENCY NAME & ADDRESS(if different from Controlling Office)	15. SECURITY CLASS. (of this report) UNCLASS
	15a. DECLASSIFICATION/DOWNGRADING SCHEDULE

16. DISTRIBUTION STATEMENT (of this Report)

APPROVED FOR PUBLIC RELEASE; DISTRIBUTION UNLIMITED

DTIC ELECTE SEP 29 1982 S D H

17. DISTRIBUTION STATEMENT (of the abstract entered in Block 20, if different from Report)

18. SUPPLEMENTARY NOTES

APPROVED FOR PUBLIC RELEASE: IAW AFR 190-17

AIR FORCE INSTITUTE OF TECHNOLOGY (ATC)
WRIGHT-PATTERSON AFB OH 45433

Lynn Wolaver
LYNN E. WOLAVER
Dean for Research and Professional Development
22 SEP 1982

19. KEY WORDS (Continue on reverse side if necessary and identify by block number)

20. ABSTRACT (Continue on reverse side if necessary and identify by block number)

ATTACHED

AD A119758

DTIC FILE COPY

DD FORM 1 JAN 73 1473 EDITION OF 1 NOV 65 IS OBSOLETE UNCLASS

82 09 28 028 SECURITY CLASSIFICATION OF THIS PAGE (When Data Entered)

ABSTRACT

In this paper diagnostics of the zonally-averaged global circulation in both isobaric and isentropic coordinates are presented. Although diagnostics for the entire FGGE year have been computed, only the results for January, April, July and October will be shown. The discussion focuses primarily on January or the Northern Hemisphere winter circulation. After a brief discussion of the data processing procedures the isobaric and isentropic mass circulations are compared. The meridional distribution of zonally-averaged diabatic heating is calculated indirectly from the isentropic meridional mass circulation. In the final portion of the results diagnostics of relative angular momentum transport in isobaric and isentropic coordinates are contrasted and the forcing of mean meridional circulations is briefly discussed.

81-34T

AFIT RESEARCH ASSESSMENT

The purpose of this questionnaire is to ascertain the value and/or contribution of research accomplished by students or faculty of the Air Force Institute of Technology (ATC). It would be greatly appreciated if you would complete the following questionnaire and return it to:

AFIT/NR
Wright-Patterson AFB OH 45433

RESEARCH TITLE: The Mass and Angular Momentum Balance of the Zonally-Averaged Global Circulation

AUTHOR: Ronald D. Townsend & Donald R. Johnson

RESEARCH ASSESSMENT QUESTIONS:

1. Did this research contribute to a current Air Force project?

( ) a. YES ( ) b. NO

2. Do you believe this research topic is significant enough that it would have been researched (or contracted) by your organization or another agency if AFIT had not?

( ) a. YES ( ) b. NO

3. The benefits of AFIT research can often be expressed by the equivalent value that your agency achieved/received by virtue of AFIT performing the research. Can you estimate what this research would have cost if it had been accomplished under contract or if it had been done in-house in terms of manpower and/or dollars?

( ) a. MAN-YEARS _____ ( ) b. $_____

4. Often it is not possible to attach equivalent dollar values to research, although the results of the research may, in fact, be important. Whether or not you were able to establish an equivalent value for this research (3. above), what is your estimate of its significance?

( ) a. HIGHLY SIGNIFICANT ( ) b. SIGNIFICANT ( ) c. SLIGHTLY SIGNIFICANT ( ) d. OF NO SIGNIFICANCE

5. AFIT welcomes any further comments you may have on the above questions, or any additional details concerning the current application, future potential, or other value of this research. Please use the bottom part of this questionnaire for your statement(s).

NAME GRADE POSITION

ORGANIZATION LOCATION

STATEMENT(s):

FOLD DOWN ON OUTSIDE - SEAL WITH TAPE

AFIT/NR
WRIGHT-PATTERSON AFB OH 45433

OFFICIAL BUSINESS
PENALTY FOR PRIVATE USE, $300

NO POSTAGE
NECESSARY
IF MAILED
IN THE
UNITED STATES

BUSINESS REPLY MAIL
FIRST CLASS PERMIT NO. 73236 WASHINGTON D.C.

POSTAGE WILL BE PAID BY ADDRESSEE

AFIT/ DAA
Wright-Patterson AFB OH 45433

FOLD IN

81-34T

THE MASS AND ANGULAR MOMENTUM BALANCE OF THE ZONALLY-AVERAGED GLOBAL CIRCULATION

Ronald D. Townsend and Donald R. Johnson
University of Wisconsin-Madison

1. Introduction

A primary objective of atmospheric general circulation research during the past three decades (e.g., Lorenz, 1967; Newell et al., 1970; Starr, 1966; Oort and Rasmusson, 1970; and others) has been to identify physical processes associated with the forcing and maintenance of the zonally-averaged global circulation. Investigators have explained the zonally-averaged global circulation and associated transports of mass, angular momentum, and energy as a response to differential heating and rotation. Virtually all general circulation research has been conducted in isobaric coordinates. However, extensive research in isobaric coordinates has failed to isolate mean circulations directly associated with planetary scale heat sources and sinks. Both the Hadley and Ferrel circulations are restricted in meridional extent from that expected from thermodynamic considerations and their maintenance depends in large part on the eddy transports of angular momentum and sensible heat (Lorenz, 1967).

Alternatively, Johnson and Dutton (see Dutton, 1976; pages 423-429) first suggested that a thermally-forced, Hadley-type meridional circulation spanning a hemisphere occurs within the isentropical zonally-averaged circulation. Limited research in isentropic coordinates (Henderson, 1971; Zillman, 1972; Callimore, 1973; and Otto, 1974) has fostered the development of an isentropic perspective of the general circulation which is intriguing and in many ways different from the isobaric perspective. The data set generated during the First GARP Global Experiment (FGGE) provides a unique opportunity

to investigate the planetary scale circulation in isobaric and isentropic coordinates.

In this paper diagnostics of the zonally-averaged global circulation in both isobaric and isentropic coordinates are presented. Although diagnostics for the entire FGGE year have been computed, only the results for January, April, July and October will be shown. The discussion focuses primarily on January or the Northern Hemisphere winter circulation. After a brief discussion of the data processing procedures the isobaric and isentropic mass circulations are compared. The meridional distribution of zonally-averaged diabatic heating is calculated indirectly from the isentropic meridional mass circulation. In the final portion of the results diagnostics of relative angular momentum transport in isobaric and isentropic coordinates are contrasted and the forcing of mean meridional circulations is briefly discussed.

2. Data processing

a. Isobaric and isentropic data

The data set used in this study is the FGGE Level IIIa data set generated by the United States National Meteorological Center (NMC) and obtained through the National Center for Atmospheric Research. The characteristics of the Level IIIa data set and NMC's optimum interpolation global data assimilation system are fully described by NMC's Staff Atmospheric Analysis Branch (1979), Fleming et al. (1979a and 1979b), Bergman (1979), and McPherson et al. (1979).

The isoberic data consists of twice daily global analysis fields for the 12 mandatory pressure levels from 1000 mb to 50 mb on a 2.5° latitude/longitude grid covering the period December 1978 through November 1979. Parameters extracted directly from the Level IIIa analyses include zonal (u) and meridional (v) wind components, temperature (T), geopotential height (z), and surface pressure.

Global isentropic fields are generated from the isobaric analyses by a vertical interpolation under the assumption of a linear variation of the pressure (p) and other parameters with $\theta^{1/\kappa}$ (θ is potential temperature and κ is the gas constant for dry air (R_d) divided by the specific heat at constant pressure (c_p)). Gridded fields of pressure, the horizontal wind components and the Montgomery stream function (ψ_M) are produced at 16 isentropic levels with 10 K vertical resolution. The vertical extent of the isentropic data may vary from Northern to Southern Hemispheres and month to month since the data is processed by hemisphere and the 16 levels analyzed depend explicitly on the minimum surface potential temperature observed during the month. The minimum vertical extent of the isentropic analyses for any given observation time is 370 K. Thus some figures may show nothing above 370 K for a given hemisphere because of this limitation.

The generalized transport equation for any property per unit mass f (Johnson and Downey, 1975a) is expressed by

$$\frac{\partial}{\partial \eta}(\rho J_\eta f) + \nabla_\eta \cdot (\rho J_\eta \underset{\sim}{U} f) + \frac{\partial}{\partial \eta}\left(\rho J_\eta \frac{d\eta}{dt} f\right) = \rho J_\eta \frac{df}{dt} \qquad (1)$$

where ρ is the density, J_η is the Jacobian $\partial z/\partial \eta$ of transformation from the vertical coordinate z to η, and $\underset{\sim}{U}$ is the horizontal velocity. The quantity

$\rho J_\eta f$ is the property within an incremental volume element $\Delta A\, \Delta\eta$ while the substantial derivative $d\eta/dt$ in combination with $\rho J_\eta f$ defines the vertical flux through quasi-horizontal surfaces of constant η . This form of the transport equation depends on the use of the meteorological convention of projection of fields from quasi-spherical surfaces of constant η onto their counterpart spherical surfaces of constant z.

The zonally-averaged transport equation is

$$\frac{\partial}{\partial t_\eta}(\overline{\rho J_\eta}^{\lambda}) + \frac{1}{a\cos\phi}\frac{\partial}{\partial\phi}(\overline{\rho J_\eta v f}^{\lambda}\cos\phi) + \frac{\partial}{\partial\eta}\left(\overline{\rho J_\eta \frac{d\eta}{dt} f}^{\lambda}\right) = \overline{\rho J_\eta \frac{d_\eta}{dt}}^{\lambda} \quad (2)$$

where a is the earth's radius and the zonal average operator and its deviation are defined for any quantity g by

$$\overline{g}^{\lambda} = \frac{1}{2\pi}\int_0^{2\pi} g\, d\lambda$$

$$g'^{\lambda} = g - \overline{g}^{\lambda} \quad . \qquad (3)$$

This form of the zonally-averaged transport equation for the circumpolar vortex provides a basic definition of the balance of a property within the closed differential tube of cross-sectional area $\Delta\phi\, \Delta\eta$ that extends zonally along constant latitude as suggested by Figure 1. The balance in (2) is between the tendency of the property within the zonal tube, the net meridional and vertical transport of the property through the surfaces of the differential tube, and the sources and sinks within.

The zonal mass-weighted average, the only operator which properly defines the mean property of the zonal tube, and its deviation are

$$\langle f \rangle^{\lambda} = \frac{\overline{\rho J_{\eta} f}^{\lambda}}{\overline{\rho J_{\eta}}^{\lambda}} \tag{4}$$

$$f^{*\lambda} = f - \langle f \rangle^{\lambda} \quad .$$

With the hydrostatic assumption zonally-averaged mass is given by

$$\overline{\rho J_{\eta}}^{\lambda} = -\frac{1}{g} \frac{\overline{\partial p}^{\lambda}}{\partial \eta} \quad , \tag{5}$$

where g is gravity.

Note that in hydrostatic isobaric coordinates with ρJ_p constant (1/g) the zonal mass-weighted average reduces to the conventional zonal isobaric average

$$\langle f \rangle^{\lambda} = \overline{f}^{\lambda} \tag{6}$$

Thus the averaging operator in (4) is applicable to both coordinate systems.

Similarly, to properly account for the tendency of ρJ_{η} and f, the time mass-weighted average of f and its deviation are defined by

$$\langle f \rangle^{t} = \frac{\overline{\rho J_{\eta} f}^{t}}{\overline{\rho J_{\eta}}^{t}} \tag{7}$$

$$f^{*t} = f - \langle f \rangle^{t}$$

where the time average of g over the period T and its deviation are

$$\overline{g}^t = \frac{1}{T} \int_0^T g \, dt \qquad (8)$$

$$g'^t = g - \overline{g}^t \quad .$$

Again $\langle g \rangle^t$ reduces to $\overline{g}^t$ in hydrostatic isobaric coordinates.

A time and zonal mass-weighted average of f through the combination of (4) and (7) is defined by

$$\langle f \rangle^{\lambda,t} = \frac{\overline{\rho J_\eta f}^{\lambda,t}}{\overline{\rho J_\eta}^{\lambda,t}} = \frac{\overline{\overline{\rho J_\eta \langle f \rangle}^{\lambda}}^{t}}{\overline{\rho J_\eta}^{\lambda,t}} \qquad (9)$$

With mass symmetry of isobaric coordinates, (9) reduces to the familiar time and space average, $\overline{f}^{\lambda,t}$.

3. The mass balance

a. Isobaric mass circulations

The mean mass circulations will be presented through the use of a mass stream function (e.g., Oort and Rasmusson, 1970). The isobaric mass stream function is computed from $\overline{v}^{\lambda,t}$ by

$$\psi_p(\phi,p) = -\frac{2\pi a \cos\phi}{g} \int_{p_{sfc}}^{p} \overline{v}^{\lambda,t} \, dp \qquad (10)$$

where ϕ is latitude, a is the earth's radius, and p_{sfc} is surface pressure.

The mass circulation is balanced at each latitude ϕ so that the integral constraint of $\psi_p(\phi, p_T)$ equal to zero is satisfied for p_T equal to 50 mb, i.e., no net mass flow is allowed across latitude circles for the layer extending from the earth's surface to 50 mb. In general this adjustment is equivalent to a correction of less than 0.25 m s^{-1} to $\overline{v}^{\lambda,t}$ at each level for any given latitude and month.

The isobaric mass circulation for January 1979 in Figure s basically consistent with the results of previous investigations (Oort Rasmusson, 1970). The strong Northern Hemisphere Hadley cell ext from 30°N to 15°S is the dominant feature. Although not evident in the figure, the maximum values of $\overline{v}^{\lambda,t}$ for the upper and lower branches of this Hadley cell are 1.4 m s^{-1} and -1.2 m s^{-1}, respectively. A weaker Southern Hemisphere Hadley cell is located between 15°S and 30°S. Indirect Ferrel cells occur in the mid-latitudes of both hemispheres. The equatorward and poleward branches of the Northern Hemisphere Ferrel circulation attain velocities of -0.7 m s^{-1} and 0.8 m s^{-1}, respectively, while the corresponding values for the Ferrel cell in the Southern Hemisphere are slightly less. A direct cell in northern high latitudes, while not well-defined, suggests a three cell structure.

The seasonal variation of the isobaric mass circulations during FGGE is evident in a comparison of the results displayed in Figures 2, 3, 4, and 5. The Hadley circulations that exist in low latitudes of both hemispheres during April and October tend to be symmetric about the equator. The winter Hadley cell for the Southern Hemisphere extends from near 30°S to 20°N and is intense, being nearly double the strength of its counterpart in the winter Northern Hemisphere. Weaker Ferrel cells persist in the middle latitudes of both hemispheres and vary seasonally in strength.

The seasonal and hemispheric variation of the mass circulation reflects the variation of the zonally-averaged meridional motion (not shown in the figures). The maximum absolute values for the upper branch of the Hadley cells range from 1.0 m s^{-1} in April and October to 1.8 m s^{-1} in July while in the lower branch $\overline{v}^{\lambda,t}$ reaches a maximum of 2.2 m s^{-1} in July. The mean meridional velocities of the upper and lower branches of the Ferrel circulations are between -1.0 and 1.0 m s^{-1} in all months. In the lower branch of the Southern Hemisphere Ferrel cell the maximum of the poleward motion ranges from -0.5 m s^{-1} in October to near -0.9 m s^{-1} in April and July. In the upper branch the maximum values are consistently near 0.5 m s^{-1} except in April when its value drops to 0.3 m s^{-1}. In the mid latitudes of the Northern Hemisphere the maximum of the zonally-averaged meridional motion in the poleward branch of the lower levels varies from 0.4 m s^{-1} in July and October to 0.8 m s^{-1} in January, while in the higher levels the largest values of the equatorward motion are near -0.3 m s^{-1} in all months except January when its value reaches -0.7 m s^{-1}.

b. Isentropic mass circulations

Within isentropic coordinates the hydrostatic mass distribution $\overline{\rho J_\theta}^{\lambda,t}$ is determined by the zonally-averaged pressure difference between two isentropic surfaces. Figure 6 shows the meridional distribution of $\overline{\rho J_\theta}^{\lambda,t}$ and $\overline{p}^{\lambda,t}$ for January and July. Most of the tropospheric mass is confined between 290 K and 360 K in tropical latitudes and between 260 K and 320 K in the mid-latitudes of the winter hemisphere. The convention that pressure on underground isentropes equals the surface pressure, used in the specification of the mass distribution, results in decreasing values of $\overline{\rho J_\theta}^{\lambda,t}$ in the lower isentropic layers. Such a decrease is not necessarily an indication of a

change in stability within the free atmosphere but reflects within the zonally-averaged distribution the mapping of longitudinal segments of the mass within cold polar air masses in conjunction with the longitudinal segments of zero mass where isentropes are contiguous with the earth's surface in warm sectors of cyclone waves. The field of $\overline{p}^{\lambda,t}$ is shown to aid in relating mean isentropic and isobaric structures.

With (5) and (9) the mean meridional motion in quasi-spherical isentropic coordinates

$$\langle v \rangle^{\lambda,t} = \frac{\overline{\rho J_\theta v}^{\lambda,t}}{\overline{\rho J_\theta}^{\lambda,t}} \tag{11}$$

is expressed by

$$\langle v \rangle^{\lambda,t} = \frac{\overline{\frac{\partial p}{\partial \theta} v}^{\lambda,t}}{\overline{\frac{\partial p}{\partial \theta}}^{\lambda,t}} \quad . \tag{12}$$

The mean geostrophic and ageostrophic components of the meridional motion are

$$\langle v \rangle^{\lambda,t} = \langle v_g \rangle^{\lambda,t} + \langle v_{ag} \rangle^{\lambda,t} \quad . \tag{13}$$

Since $\overline{v_g}^{\lambda}$ is identically zero, the mass-weighted, zonally-averaged geostrophic component

$$\langle v_g \rangle^{\lambda,t} = \frac{\overline{\frac{\partial p}{\partial \theta} v_g}^{\lambda,t}}{\overline{\frac{\partial p}{\partial \theta}}^{\lambda,t}} = \frac{\overline{\frac{\partial p}{\partial \theta}' v_g'}^{\lambda,t}}{\overline{\frac{\partial p}{\partial \theta}}^{\lambda,t}} \tag{14}$$

exists in isentropic coordinates through the covariance of the mass (an inverse static stability measure) and the meridional geostrophic motion. The isobaric counterpart to this mode is identically zero.

Some physical insight into mean meridional motion within the isentropic structure is provided by Johnson (1979) through contrasting the structure of steady and amplifying mid-latitude baroclinic waves.

In the schematic of the horizontal distribution of geopotential and potential temperature of the steady baroclinic wave (Figure 7a), the geopotential and temperature waves are assumed to be in phase. Within the zonal vertical cross-section of a layer extending from a lower isentropic surface θ_ℓ to an upper isentropic surface θ_u, a midvalue isentropic surface θ_m (e.g., θ_m = 290 K) divides the hypothetical atmosphere into two regions. In the cross-section, the dotted vertical lines designate trough and ridge positions that separate regions of poleward and equatorward geostrophic motion.

With a vertical scale linear in pressure, the relative position of the isentrope shows the greater mass (g^{-1} ($\partial p/\partial\theta$) $d\theta$) in the layer between θ_ℓ and θ_m to be positioned in the trough and lesser mass to be located in the ridge. The reverse mass distribution occcurs in the layer above θ_m. With the in-phase relation of the potential temperature and geopotential fields, the isentropic mass transport $\rho J_\theta v$ is symmetric about the trough line within each layer. The poleward mass transport by the geostrophic mode forward of the trough is exactly balanced by equatorward transport to the rear of the trough. Thus the mean meridional geostrophic mass transport vanishes within each layer.

In the traditional model (Charney, 1947; Eady, 1949) of an amplifying baroclinic wave (Figure 8a), the potential temperature wave is assumed to lag the geopotential wave by a phase angle 90°. In the zonal cross-section, this

lag of potential temperature introduces a westward tilt of the baroclinic wave. A systematic structure results which provides for poleward geostrophic mass transport above 290 K and an equatorward mass transport below 290 K. Poleward motion ahead of the trough and above 290 K is located within a deeper layer of mass than in the rear of the trough with its equatorward motion. Beneath 290 K the reverse occurs with more mass moving equatorward in the rear of the trough than ahead of the trough. Consequently, the mean geostrophic mass transport of active baroclinic waves within this two-layered structure is poleward above 290 K and equatorward below 290 K. Thus the components of geostrophic mass transport provide a degree of freedom for poleward and equatorward branches of a meridional circulation in the isentropic zonally-averaged structure that do not exist within the isobaric structure. Some aspects of the degrees of freedom for the mean mass transport within azimuthally-averaged motion of vortices are discussed by Johnson and Downey (1975 a and b). In this application to the circumpolar vortex, azimuthal averaging corresponds to zonal averaging and divergent and non-divergent modes correspond to ageostrophic and geostrophic modes, respectively, since the coriolis parameter is independent of longitude.

The isentropic mass stream function as a function of ϕ and θ is defined by

$$\psi_\theta(\phi,\theta) = 2\pi a \cos\phi \int_{\theta_B}^{\theta} \overline{\rho J_\theta}^{\lambda,t} \langle v \rangle^{\lambda,t} \, d\theta \quad , \qquad (15)$$

where θ_B is the minimum isentropic level of the time averaging period. As in isobaric coordinates the isentropic mass circulations are balanced so that

$\psi_\theta(\phi,\theta_T)$ is zero for any ϕ and θ_T equal to the top level of the isentropic data. This adjustment equates to corrections in $\langle v\rangle^{\lambda,t}$ similar in magnitude to that of $\overline{v}^{\lambda,t}$ discussed previously.

The isentropic mean meridional circulation in January (Fig. 2) reveals a large Hadley-type circulation extending throughout the entire Northern Hemisphere to 15°S. The vertical branches forced by planetary scale heat sources and sinks show mean upward diabatic mass transport in tropical latitudes and downward mass transport in polar latitudes. The poleward branch linking tropical and polar latitudes within this mass circulation is located primarily between the 310 K and 360 K surfaces in low latitudes with the maximum meridional motion ($\langle v\rangle^{\lambda,t}$) being slightly greater than 1.0 m s^{-1} near 350 K in the 0°-5°N region. In higher latitudes this branch is located within the 290 K to 320 K isentropic layer where $\langle v\rangle^{\lambda,t}$ reaches a value of 1.2 m s^{-1}. The equatorward branch of the Hadley-type circulation extends from Northern Hemisphere polar latitudes to the tropical regions of the Southern Hemisphere and lies beneath the poleward branch. This branch is displaced upward to higher isentropic layers in lower latitudes due in part to energy sources through sensible heat transfer from the ocean to the atmosphere. Implicit in the tilt of the quasi-horizontal branches of these mass circulations is some thermal forcing of the upward and downward mass transport occurring during meridional exchange.

The geostrophic mass stream function computed by substituting $\langle v_g\rangle^{\lambda,t}$ for $\langle v\rangle^{\lambda,t}$ in (15) is shown poleward of 10° in each hemisphere in each of the figures. The mean mode of geostrophic mass transport is confined primarily to extratropical latitudes and is embedded within the structure of baroclinic waves. Figure 2 shows a strong, direct geostrophic mass circulation in the Northern Hemisphere winter while the geostrophic circulation of the Southern

Hemisphere is much weaker. Typical values of $\langle v_g \rangle^{\lambda,t}$ range from 1.5 to 1.8 m s^{-1} in the poleward branch of the northern circulation. The forcing of the geostrophic mode of poleward and equatorward meridional mass transport occurs primarily through respective negative and positive pressure torques (Johnson and Downey, 1975b; Gallimore and Johnson, 1977), within upper and lower branches of the mass circulation in mid-latitudes.

The ageostrophic component of the isentropic mass circulations in Figure 2, computed with $\langle v_{ag} \rangle^{\lambda,t}$ in (15), reveals a direct Hadley circulation in low latitudes and an indirect Ferrel circulation in mid-latitudes. A comparison of the ageostrophic mass circulations in isobaric (in isobaric coordinates $\overline{v}^{\lambda,t}$ is identical with $\overline{v_{ag}}^{\lambda,t}$) and isentropic coordinates shows the remarkable similarity in both the position and intensity for each of the Hadley and Ferrel cells. The mean ageostrophic meridional velocities in the upper and lower branches of the low latitude Hadley cell are 1.3 m s^{-1} and -1.3 m s^{-1}, respectively, which are close to the corresponding isobaric values of $\overline{v}^{\lambda,t}$ (1.4 m s^{-1} and -1.2 m s^{-1}) presented earlier. The respective maximum values of $\langle v_{ag} \rangle^{\lambda,t}$ in the equatorward and poleward branches of the Northern Hemisphere isentropic Ferrel circulations are -0.7 m s^{-1} and 0.9 m s^{-1}. These values also compare favorably with those given for the corresponding isobaric Ferrel circulation (-0.7 m s^{-1} and 0.8 m s^{-1}). Comparison of the mean ageostrophic meridional velocities in isentropic and isobaric coordinates yields similar results for the Southern Hemisphere Ferrel cell.

The seasonal variation of the isentropic mass circulations is evident in Figures 2, 3, 4 and 5. In April and October the isentropic Hadley-type circulations span both the Northern and Southern Hemispheres. The geostrophic mode dominates in extratropical latitudes. In July the strong Hadley-type circulation that extends from the high southern latitudes to near 20°N is in

part associated with the Asiatic summer monsoon. Its Northern Hemisphere counterpart in July is weak. During all months the isentropic ageostrophic circulations display patterns similar to the isobaric low-latitude Hadley and mid-latitude Ferrel circulations. The similarity of isentropic and isobaric ageostrophic mass circulations in atmospheric domains with mass structures that tend to be symmetric about the axis of rotation is to be expected from the analysis of Johnson and Downey (1975) since the geostrophic mode of mass transport would tend to vanish. Such is the case in tropical latitudes. The similarity of the ageostrophic modes in domains with longitudinal variations of mass could not be isolated in the earlier analysis since in isentropic coordinates a degree of freedom exists for differences associated with the statistic $\overline{(\rho J_\theta)^* v_{ag}^*}^\lambda$. This statistic vanishes if the zonal variations of mass and ageostrophic meridional motion are not correlated. Although this has not been ascertained in the preliminary analyses, the remarkable similarity of the isobaric and isentropic mean meridional ageostrophic motion suggests that the covariance is minimal. Given the relatively large value of mean ageostrophic meridional motion in comparison with the mean geostrophic motion in isentropic coordinates, it is not readily apparent that the Ferrel circulation can be viewed as a secondary circulation within the zonally-averaged structure.

4. Meridional distribution of diabatic heating

The poleward and equatorward branches of the isentropic mean Hadley-type meridional circulations link vertical branches associated with planetary scale heat sources and sinks. Implicit in these mass circulations is the thermal forcing of upward and downward mass transport through atmospheric stratification by differential diabatic heating. Through the continuity rela-

tionship the meridional and vertical distribution of the mean diabatic heating can be determined indirectly from the meridional mass transport.

Diabatic heating is computed in the coordinate system (λ, a sin ϕ, θ) in order to express the zonally-integrated structure by equal incremental volumes and equalize the uncertainty. Thus the inferred heating rates become mass-weighted, time and zonal averages representing equal areal increments of the atmosphere. For simplicity these values are referred to as zonally-averaged diabatic heating.

Mass-weighted, zonally-averaged distributions of total diabatic heating for four months of FGGE are shown in Figure 9. In January the heating maximum that is undoubtedly associated with the moist convection of the Intertropical Convergence Zone (ITCZ) is captured quite nicely near 15°S with values of near 1.0 K day^{-1} at 330 K. An important secondary heat source appears in middle latitudes in association with sensible and latent energy added within mid-latitude cyclonic circulations. The heating of near 2.0 K day^{-1} that occurs in the lowest isentropic layers is in all probability associated with the strong sensible heat transfer from the ocean to the atmosphere eastward of the Asian and North American continents. Downward mass transport of the higher latitudes and the higher layers is associated with the excess of loss of energy through emission of long wave radiation over other processes of heat addition. The cooling in polar regions exceeds -1.0 K day^{-1} in the northern polar region.

Seasonal variations in the location and strength of the large scale heat sources and sinks are evident from the profiles in Figure 9. Heating of the tropics and the lower layers of the northern mid-latitudes persists in April and October. Consistent with the intense mass circulation of July is the strong net diabatic heating in the Northern Hemisphere tropics and net

cooling in the Southern Hemisphere tropics. With the latent heating of the ITCZ, particularly the summer Asian Monsoon in the Northern Hemisphere, zonally-averaged heating of over 1.0 K day^{-1} occurs throughout a deep layer from 310 K to 330 K near 10°N. The tropical region of the Southern Hemisphere is dominated by diabatic cooling which must be attributable to strong infrared radiation emission and also possibly evaporative processes associated with the extensive clouds that are advected from adjacent regions of the deep convection associated with the monsoon. Loss of energy through infrared radiation is maximized in these regions through the combination of a dry troposphere overlying a warm, moist and partially cloudy lower atmosphere beneath the trade wind inversion.

Meridional profiles of vertically and zonally-averaged total diabatic heating are presented in Figure 10. The vertical averages in Figure 10 are mass-weighted and take into account heating or cooling over a variable depth of the atmosphere determined by the isentropic mass distribution (e.g., Fig. 6). These profiles primarily reflect the latitudinal distribution of the dominant features and physical processes emphasized in the preceding discussion. As expected the maximum of heating in tropical latitudes shifts seasonally and is largest in the Northern Hemisphere tropics of its summer season. The heating maximum in mid-latitudes is most pronounced and organized in January and April. During July and October mid-latitude heating is composed of two relatively smaller but distinct maximums. Such features are much less pronounced in the Southern Hemisphere mid-latitudes due in part to the lack of a continent-ocean contrast within the westerlies that provides for the oceanic latent and sensible energy supply through frequent cold outbreaks over relatively warm oceans.

5. Angular momentum balance

a. Isobaric coordinates

The zonal wind profiles $\overline{u}^{\lambda,t}$ and the averaged meridional transport of relative angular momentum during FGGE are also similar to previous results (Lorenz, 1967; Oort and Rasmusson, 1970; and others). The time and zonally-averaged u-component for January and July is presented in Figure 11. In January strong westerlies dominate both hemispheres with weak tropical easterlies in the lower troposphere. In July the Southern Hemisphere westerlies are stronger and display two maxima: one at 30°S near 200 mb and the other near 60°S above 100 mb. Easterly winds dominate the tropical latitudes while the westerlies in northern latitudes are substantially weaker in July.

The transport of relative angular momentum across a latitude ϕ is given by

$$F_p(\phi) = -\frac{2\pi a^2 \cos^2\phi}{g} \int_{p_{sfc}}^{p_T} \overline{uv}^{\lambda,t}\, dp \quad . \tag{16}$$

The transport in (16) is also partitioned into the three components

$$\overline{uv}^{\lambda,t} = \overline{u}^{\lambda,t}\,\overline{v}^{\lambda,t} + \overline{u^{*t}{}^{\lambda}\, v^{*t}{}^{\lambda}}^{\lambda,t} + \overline{u^{*t}\, v^{*t}}^{\lambda,t} \quad , \tag{17}$$

representing the transport by the mean meridional circulation, standing eddies, and transient circulations, respectively. Figures 12 and 13 display the vertical and meridional distribution of relative angular momentum trans-

port for January and July. Vertically-integrated profiles of isobaric angular momentum transport are shown in Figure 14.

In isobaric coordinates the transient component is the dominant mode of angular momentum transport in January. It is poleward at virtually all latitudes in each hemisphere. The standing eddy transport is significant in northern subtropical and middle latitudes while the mean meridional transport by the Hadley cell is important in low latitudes only. Angular momentum transport in July reveals a similar picture. Poleward transport by transient and mean meridional circulations dominates the middle and low latitudes, respectively, of the Southern Hemisphere. The lack of a land-ocean contrast in the extratropical latitudes of the Southern Hemisphere appears to restrict transport by the standing eddies to a relatively minor role.

b. Isentropic coordinates

In contrasting the results from isobaric and isentropic analyses, it is important to realize that the vertically-integrated transport of an atmospheric property across a latitudinal boundary of the circumpolar vortex must remain invariant with respect to different coordinate systems. However, the mean and eddy transport modes within a vortex with zonal asymmetries are coordinate dependent (Johnson and Downey, 1975a). Conceptually, an isentropic mean meridional circulation spanning the hemisphere could provide the required poleward angular momentum transport. Before addressing this point, it is interesting to contrast the zonally-averaged velocity and momentum structures of isobaric and isentropic coordinates.

The isentropic structure of the average zonal wind $\langle u \rangle^{\lambda,t}$ for January and July are presented in part of Figure 15. Its structure is similar to its isobaric counterpart in Figure 11. The comparison is limited only by the

vertical extent of the isentropic data. The isentropic structure of the zonally-averaged momentum component ($\overline{\rho J_\theta u}^{\lambda,t}$ or $\overline{\rho J_\theta}^{\lambda,t}\ \langle u\rangle^{\lambda,t}$) shown in part of Figure 15 presents an interesting contrast with the average zonal wind. Distinct momentum cores appear in the isentropic structure for January and July. This latter momentum distribution ($\overline{\rho J_\theta}^{\lambda,t}\ \langle u\rangle^{\lambda,t}$) reflects the larger mass located in the middle isentropic layers and lesser mass in lower and higher isentropic layers.

In isentropic coordinates the vertically-integrated transport of relative angular momentum across a latitude ϕ is expressed by

$$F_\theta(\phi) = 2\pi a^2 \cos^2\phi \int_{\theta_B}^{\theta_T} \overline{\rho J_\theta}^{\lambda,t}\ \langle uv\rangle^{\lambda,t}\, d\theta \qquad (18)$$

and shown in Figure 14 for comparison with the isobaric results. Similar to (17) the transport in (18) partitioned into

$$\langle uv\rangle^{\lambda,t} = \langle u\rangle^{\lambda,t}\ \langle v\rangle^{\lambda,t} + \langle\langle u\rangle^{t*\lambda}\ \langle v\rangle^{t*\lambda}\rangle^{\lambda} + \langle u^{*t}\ v^{*t}\rangle^{\lambda,t} \qquad (19)$$

represents transport by mean meridional, standing eddy, and transient circulations. The vertical and meridional distribution of relative angular momentum transport by the three components is given for January and July in Figures 16 and 17.

The vertically-integrated total transport of relative angular momentum for January in Figure 14 is virtually identical in isentropic and isobaric coordinates. In addition vertically-integrated transport by the standing eddies is nearly the same in both coordinate systems. Mean angular momentum transport by the isentropic, hemispheric Hadley-type circulation is poleward at all northern latitudes, while the mean poleward transport is confined to

low latitudes in isobaric coordinates. The results in isentropic coordinates show that the transient circulations also accomplish a major portion of the poleward momentum transport. However, in higher latitudes of the Northern Hemisphere the isentropic transient transport is less than the isobaric transient. With the total and standing eddy components nearly equal in isobaric and isentropic coordinates and the mid-latitude isobaric mean transport almost negligible, the angular momentum transport by isobaric transient circulations tends to equal the transport by isentropic mean meridional plus transient circulations in extratropical latitudes.

Within the isobaric perspective of the general circulation standing and transient eddies are the dominant means of angular momentum transport in mid-latitudes. The isentropic perspective has the additional degree of freedom for a mean geostrophic mode of transport associated with hemispheric mean meridional circulations which accounts for some angular momentum transport. This isentropic mean meridional motion in mid-latitudes is likely realized through the structure of amplifying baroclinic waves (Johnson, 1979). Since amplifying baroclinic waves are generally transient, the isentropic transport by both the mean meridional and transient modes as well as the transient isobaric mode are probably associated with active baroclinic waves in mid-latitudes. Thus active baroclinic waves in mid-latitudes become the phenomena which link the transient angular momentum transport in isobaric coordinates with the mean and transient modes in isentropic coordinates. It is important to recognize that the meridional branches of the geostrophic mean circulation in mid-latitudes develop to satisfy balance requirements associated with the vertical diabatic mass flux. Thus, the mean geostrophic mode of angular momentum transport in isentropic coordinates that occurs through active baroclinic waves is directly linked with the mass flux associated with

diabatic heating, i.e., a thermally-forced component. This thermally-forced component of angular momentum transport, isolated through the use of isentropic diagnostics, is apparently linked to the transient component of angular momentum transport in isobaric coordinates within the phenomena of active baroclinic waves.

Johnson and Downey (1975a) emphasize that statistical partitioning of transport processes in isobaric and isentropic coordinates may yield different results for the component modes of transport due to inherent symmetric or asymmetric structures of the mass distribution within the respective coordinate systems. The differences in the statistics presented in these results substantiate that mean and eddy transport modes are coordinate dependent. These differences do not stem from a non-uniqueness of atmospheric structure but emerge from a non-uniqueness of statistics computed in different coordinate systems, i.e., the mean and deviation of physical variables and processes are determined from integration over portions of the atmosphere in one coordinate system which are not identical with the counterpart in the zonally-averaged structure of another coordinate system.

6. Forcing of mean meridional circulations

The forcing of mean meridional circulations within the circumpolar vortex has been isolated through the application of Eliassen's perspective. Eliassen (1951) shows that in a hydrodynamically stable vortex a heat source (sink) forces motion upward (downward) through isentropic stratification along a surface of constant absolute angular momentum toward lower (higher) pressure and a source (sink) of angular momentum or a positive (negative) torque forces motion along an isentropic surface away from (towards) the axis of rotation.

Kuo (1956) demonstrated that the existence of the Hadley and Ferrel circulations in isobaric coordinates can be explained only by considering the convergence (divergence) of the large-scale eddy transport of sensible heat and angular momentum as sources (sinks) of heat and angular momentum, respectively.

The results of a mean, Hadley-type meridional circulation in isentropic coordinates elucidates the dominance of a mean geostrophic mode of mass transport in mid-latitudes and an ageostrophic mode in low latitudes. The mean geostrophic circulation is explicitly related to pressure torques. Poleward geostrophic mass transport within a vortex occurs in conjunction with negative pressure torques, while equatorward geostrophic mass transport occurs with positive pressure torques. Over a uniform earth surface the sum of the negative torques must be equal and opposite to the sum of the positive pressure torques. At the same time angular momentum is transferred from the branch of a circulation with poleward geostrophic motion to the branch with equatorward geostrophic motion through the isentropic stratification by the action of pressure torques and pressure stresses (Johnson and Downey, 1975b; Johnson, 1980). Within the asymmetric wave regime of extratropical latitudes the mass-weighted zonally-averaged pressure gradient force yields a net negative torque in the upper isentropic layers and a net positive torque in lower layers. In mid-latitudes the upper poleward branch of the mean meridional circulation is forced by this negative pressure torque while the equatorward branch of lower isentropic layers is forced by the dominance of a positive pressure torque over a negative friction torque (Gallimore and Johnson, 1977). In low latitudes with its lack of geostrophy a positive friction torque associated with the low level easterlies forces equatorward ageostrophic motion in

lower layers that links with the equatorward geostrophic motion of mid-latitudes. Divergence of the eddy transport of angular momentum acts as a negative torque in the upper isentropic layers of the subtropics and forces ageostrophic poleward motion which links with the upper geostrophic branch of mid-latitudes.

The vertical branches of the isentropic mean mass circulation are forced explicitly by diabatic heating. Emission of long wave radiation in polar regions forces downward mass transport while latent energy release associated with moist convection forces upward mass transport in tropical regions. The upward vertical branch of the mid-latitude mean geostrophic circulation is forced by sensible heating in the boundary layer and latent heat release associated with extratropical cyclones. In isentropic coordinates the eddy transport of heat is not an explicit forcing term since the mass-weighted zonally-averaged transport of energy (sensible heat plus potential energy) in mid-latitudes is accomplished by the thermally-forced, mean meridional circulation.

7. Summary

A diagnostic study of the mass, angular momentum, and energy balance of the global circulation for the FGGE year has been initiated using the Level IIIa data set generated by NMC. No attempt was made to assess the quality or the impact of special FGGE data with respect to an objective analysis scheme. Even with the increased amount of real time data available during FGGE, the quantity of data from the Southern Hemisphere is probably not adequate to resolve the circulation features of the southern latitudes to a degree comparable to the Northern Hemisphere. Until the Level IIIb data set is processed, the Level IIIa fields are most likely the best global analyses available. In

addition, the FGGE Level IIIa data set provides a common base for a diagnostic study of the global circulation in both isobaric and isentropic coordinates.

The preliminary results presented in this paper are limited to mass and angular momentum transport diagnostics of the time and zonally-averaged circulation in isobaric and isentropic coordinates. A more extensive analysis of the complete mass, momentum and energy balance of the global circulation is in progress. From the results to date the contrast of energy (sensible heat plus potential energy) transport confirms the importance of both mean and eddy transport modes in isobaric coordinates while revealing that the mean mode of energy transport within the zonally-averaged isentropic structure is of primary importance.

Recognizing the added dimensions for views of the balance of the general circulation provided by a time-averaged circulation mean and transient decomposition of transport processes (Blackmon et al., 1977; Lau, 1978; Lau et al., 1978), time-averaged isobaric and isentropic statistics have also been computed and analyses have been initiated. Preliminary diagnostic results of three-dimensional, time-averaged mass circulations in isentropic coordinates are presented in a companion paper by Johnson and Townsend (1980). Future work will focus on resolving the three-dimensional structure of standing and transient modes of transport within the isentropic framework.

Diagnostics of the mass and angular momentum balance of the time and zonally-averaged global circulation for the FGGE year support the current perspective of the general circulation in isobaric coordinates. The isobaric mean meridional circulations include low latitude Hadley and mid-latitude Ferrel circulations forced in part by the eddy transport of heat and angular momentum. The required poleward transport of angular momentum is provided primarily by a mean meridional circulation in low latitudes and transient and

standing eddy circulations in middle latitudes. These diagnostics reinforce the perspective that active baroclinic waves are the dominant transport mechanism in extratropical latitudes of the zonally-averaged circulation.

The perspective of the forcing and maintenance of the zonally-averaged circumpolar vortex evolving within an isentropic framework is fundamentally different. The zonally-averaged diabatic heating distribution calculated from the isentropic mean meridional circulation reveals realistic seasonal variations in the strength and location of heat sources and sinks of the zonally-averaged atmosphere. Isentropic mean mass circulations explicitly link planetary scale heat sources and sinks and display a scale of atmospheric response that is directly determined by the scale of thermodynamic forcing. The mean geostrophic mode of mass transport occurring within the wave regime is a component of the response to large scale differential heating. Thus active baroclinic waves which reveal mean geostrophic transport of mass and energy as primary transport modes become a phenomena of response directly linked with differential heating. The strength of the isentropic mass circulation, the intensity of the circumpolar vortex, and the degree of differential heating are all explicitly related in isentropic coordinates.

The diagnostic results of angular momentum transport in isentropic coordinates show that transport by the isentropic mean meridional circulation is also important in both middle and low latitudes and combines with standing eddy and transient modes to provide the observed balance. Zonally- and vertically-integrated angular momentum transport profiles suggest that angular momentum transport by the transient mode in isobaric coordinates in middle latitudes is linked to angular momentum transport by both thermally-forced, mean meridional and transient modes in isentropic coordinates within the structure of amplifying mid-latitude baroclinic waves. The results verify

that the role of mean and eddy transport modes is coordinate dependent. Within the isentropic framework the relative modes of transport of angular momentum also differ between Northern and Southern Hemispheres. The isentropic structure of mean meridional and transient transport of angular momentum has not been completely resolved and requires further investigation. Angular momentum balance is achieved through a combination of processes which entail global scale thermally-forced transport processes, boundary conditions and non-linear interaction within the baroclinic wave domain of middle latitudes. Insight into interaction of mid-latitude baroclinic waves with embedded transient extratropical cyclones and larger scale transport processes remains a challenge within the isentropic perspective of the forcing and maintenance of the circumpolar vortex.

Acknowledgments

We express our appreciation to Mr. Thomas Whittaker and Mr. Richard Selin for their computer programming and data processing assistance and to Mr. John Stremikis for his guidance in preparing the figures. This research was supported by The National Science Foundation, Atmospheric Research Section Grant #ATM77-22976, and Climate Dynamics Research Section Grant #ATM78-22384. The first author (Capt Ronald D. Townsend) is pleased to acknowledge the research opportunity provided by the U. S. Air Force Institute of Technology.

References

Bergman, K. H., 1979: A multivariate optimum interpolation analysis system of temperature and wind fields. Mon. Wea. Rev., Vol. 107, 1423-1444.

Blackmon, M. L., J. M. Wallace, N.-C. Lau, and S. L. Mullen, 1977: An observational study of the Northern Hemisphere wintertime circulation. J. Atmos. Sci., Vol. 34, 1040-1053.

Charney, J. G., 1947: The dynamics of long waves in a baroclinic westerly current. J. Meteor., Vol. 4, 135-162.

Dutton, J. A., 1976: The Ceaseless Wind, New York, McGraw-Hill, 579 pp.

Eady, E. T., 1949: Long waves and cyclone waves. Tellus, Vol. 1, No. 3, 35-42.

Eliassen, A., 1951: Slow thermally or frictionally controlled meridional circulation in a circular vortex. Astrophys. Norv., Vol. 5, 19-60.

Fleming, R. J., T. M. Kaneskige, and W. E. McGovern, 1979a: The Global Weather Experiment I. The observational phase through the first special observing period. Bull. Am. Meteorol. Soc., Vol. 60, 649-659.

Fleming, R. J., T. M. Kaneskige, W. E. McGovern, and T. E. Bryan, 1979b: The Global Weather Experiment II. The second special observing period. Bull. Am. Meteorol. Soc., Vol. 60, 1316-1322.

Gallimore, R. G., 1973: A diagnostic model of the zonally averaged circulation in isentropic coordinates. Ph.D. Thesis, Univ. of Wisconsin, Madison, Wi., 294 pp.

Gallimore, R. G. and D. R. Johnson, 1977: The forcing of the meridional circulation of the isentropic zonally averaged circumpolar vortex. Scientific Report to NSF. Isentropic numerical models: Results on model development for zonally averaged and secondary circulations. Dept. of Meteor. and SSEC, Univ. of Wisconsin, Madison, Wi., 89-126.

Henderson, H. W., 1971: The atmospheric energy budget in isentropic coordinates. M. S. Thesis, Pennsylvania State Univ., University Park, Pa., 78 pp.

Johnson, D. R. and W. K. Downey, 1975a: Azimuthally averaged transport equations for storms: Quasi-Lagrangian diagnostics 1. Mon. Wea. Rev., Vol. 103, 697-979.

Johnson, D. R. and W. K. Downey, 1975b: The absolute angular momentum of storms: Quasi-Lagrangian diagnostics 2. Mon. Wea. Rev., Vol. 103, 1063-1076.

Johnson, D. R., 1979: Systematic stratospheric-tropospheric exchange through quasi-horizontal transport processes within active baroclinic waves. WMO Symposium on Long-Range Transport of Pollutants and its Relation to General Circulation Including Stratospheric/Tropospheric Exchange Processes, October 1-5, 1979, Sofia, Bulgaria.

Johnson, D. R., 1980: A generalized transport equation for use in meteorological coordinate systems. Mon. Wea. Rev., Vol. 108, No. 6, pp. 682-703.

Johnson, D. R., and R. D. Townsend, 1980: Dianostics of the heat sources and sinks of the Asiatic monsoon and the thermally forced planetary scale response. Paper presented at the International Conference on Preliminary FGGE Results, June 23-27, 1980, Bergen, Norway.

Kuo, H.-L., 1956: Forced and free meridional circulations in the atmosphere. J. Meteor., Vol. 13, 561-568.

Lau, N.-C., H. Tennekes, and J. M. Wallace, 1978: Maintenance of the momentum flux by transient eddies in the upper troposphere. J. Atmos. Sci., Vol. 35, 139-147.

Lau, N.-C., 1978: On the three-dimensional structure of the observed transient eddy statistics of the Northern Hemisphere winter-time circulation. J. Atmos. Sci., 35, 1900-1923.

Lorenz, E. N., 1967: The Nature and Theory of the General Circulation of the Atmosphere, WMO, Geneva, No. 218, 161 pp.

McPherson, R. D., K. H. Bergman, R. E. Kistler, G. E. Rasck, and D. S. Gordon, 1979: The NMC operational global data assimilation system. Mon. Wea. Rev., Vol. 107, 1445-1461.

NMC Staff Atmospheric Analysis Branch, 1979: Characteristics of FGGE Level IIIa data sets from the NMC global data assimilation system. AMS Preprint Volume, Fourth Conference on Numerical Weather Prediction, October 29-November 1, 1979, Silver Spring, Maryland, pp. 331-334.

Newell, R. E., D. G. Vincent, T. D. Dopplick, and D. Farruza, 1970: The energy balance of the global atmosphere. The Global Circulation of the Atmosphere, Royal Meteorological Society, London, 255 pp.

Oort, A. H. and E. M. Rasmusson, 1970: On the annual variation of the monthly mean meridional circulation. Mon. Wea. Rev., Vol. 98, 423-442.

Otto, B. L., 1974: Isentropically time-averaged mass circulations in the Northern Hemisphere. M.S. Thesis, Univ. of Wisconsin, Madison, Wi., 95 pp.

Starr, V. P. (Director), 1966: Observational studies of the atmospheric general circulation. Planetary Circulations Project, Scientific Report No. 2, A collection of papers compiled by V. P. Starr and B. Saltzman, 700 pp.

Zillman, J. W., 1972: Isentropically time-averaged mass circulations in the Southern Hemisphere. Ph. D. Thesis, Univ. of Wisconsin, Madison, Wi., 205 pp.

Figure Legends

Figure 1. Schematic of closed differential tube of cross-sectional area $d\phi d\eta$.

Figure 2. Mass stream function for the isobaric and isentropic mean meridional circulations for January 1979 (units, 10^{10} kg s^{-1}). Arrows indicate the direction of the circulation.

Figure 3. Mass stream function for the isobaric and isentropic mean meridional circulations for April 1979 (units, 10^{10} kg s^{-1}). Arrows indicate the direction of the circulation.

Figure 4. Mass stream function for the isobaric and isentropic mean meridional circulations for July 1979 (units, 10^{10} kg s^{-1}). Arrows indicate the direction of the circulation.

Figure 5. Mass stream function for the isobaric and isentropic mean meridional circulations for October 1979 (units, 10^{10} kg s^{-1}). Arrows indicate the direction of the circulation.

Figure 6. Meridional cross-sections of time and zonally-averaged pressure on an isentropic surface for January(a) and July(b) of 1979 (units, 10^2 mb) and time and zonally-averaged hydrostatic mass distribution ($\overline{\rho J}_\theta$) for January(c) and July(d) of 1979 (units, 10 kg m^2 K^{-1}).

Figure 7. Schematics of horizontal (λ,ϕ) and vertical (λ,p) distributions of geopotential and potential temperature within a steady baroclinic wave. In the zonal, vertical cross-section the dashed lines designate trough and ridge positions which separate regions of poleward and equatorward geostrophic motion within two isentropic layers. The layer in 7b extends from a lower isentrope θ_l to an intermediate isentrope θ_m to an upper isentrope θ_u (figure after Johnson, 1979).

Figure 8. Schematic of amplifying baroclinic wave, see legend of Figure 7 for structural details (figure after Johnson, 1979).

Figure 9. Meridional cross-sections of mass-weighted, time and zonally-averaged diabatic heating for January, April, July, and October 1979 (units, 10^{-1} K day^{-1}).

Figure 10. Mass-weighted vertical average of time and zonally-averaged diabatic heating for January, April, July, and October 1979 (units, K day^{-1}).

Figure 11. Meridional cross-sections of time and longitudinally-averaged zonal wind component ($\bar{u}$) in isobaric coordinates for January and July 1979 (units, m s^{-1}).

Figure 12. Meridional cross-sections of the total, mean meridional, standing eddy, and transient transport of relative angular momentum in isobaric coordinates for January 1979 (units, 10^{16} kg m^2 s^{-2} mb^{-1}).

Figure 13. Meridional cross-sections of the total, mean meridional, standing eddy, and transient transport of relative angular momentum in isobaric coordinates for July 1979 (units, 10^{16} kg m^2 s^{-2} mb^{-1}).

Figure 14. Meridional profiles of vertically integrated transport of total relative angular momentum and its component parts for January and July 1979 in isobaric coordinates(a and b) and isentropic coordinates(c and d) (units, 10^{19} kg m^2 s^{-2}).

Figure 15. Meridional cross-sections of mass-weighted, time and longitudinally-averaged zonal wind component, $\hat{u}$, (a and b) in isentropic coordinates (units, m s^{-1}) and time and longitudinally-averaged momentum, $\overline{\rho J_\theta u}$, (c and d) in isentropic coordinates for January and July 1979 (units, 10^2 (kg m s^{-1}) m^{-2} K^{-1}).

Figure 16. Meridional cross-sections of the total, mean meridional, standing eddy, and transient transport of relative angular momentum in isentropic coordinates for January 1979 (units, 10^{17} kg m^2 s^{-2} K^{-1}).

Figure 17. Meridional cross-sections of the total, mean meridional, standing eddy, and transient transport of relative angular momentum in isentropic coordinates for July 1979 (units, 10^{17} kg m^2 s^{-2} K^{-1}).

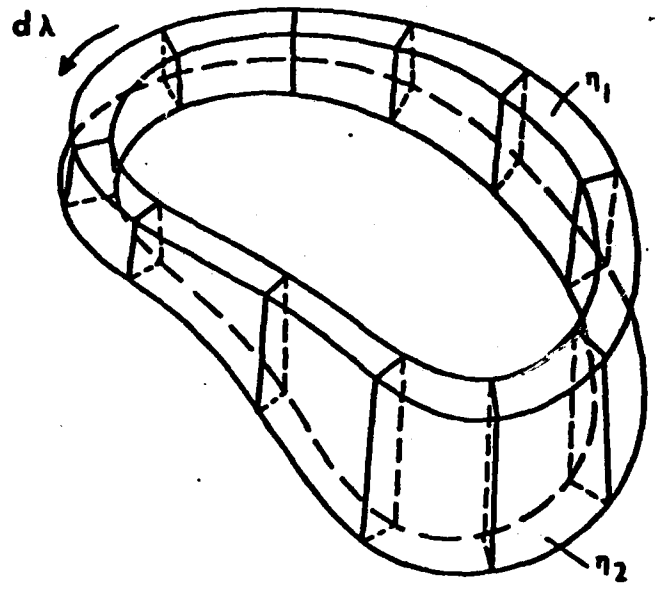

Figure 1. Schematic of closed differential tube of cross-sectional area $d\phi d\eta$.

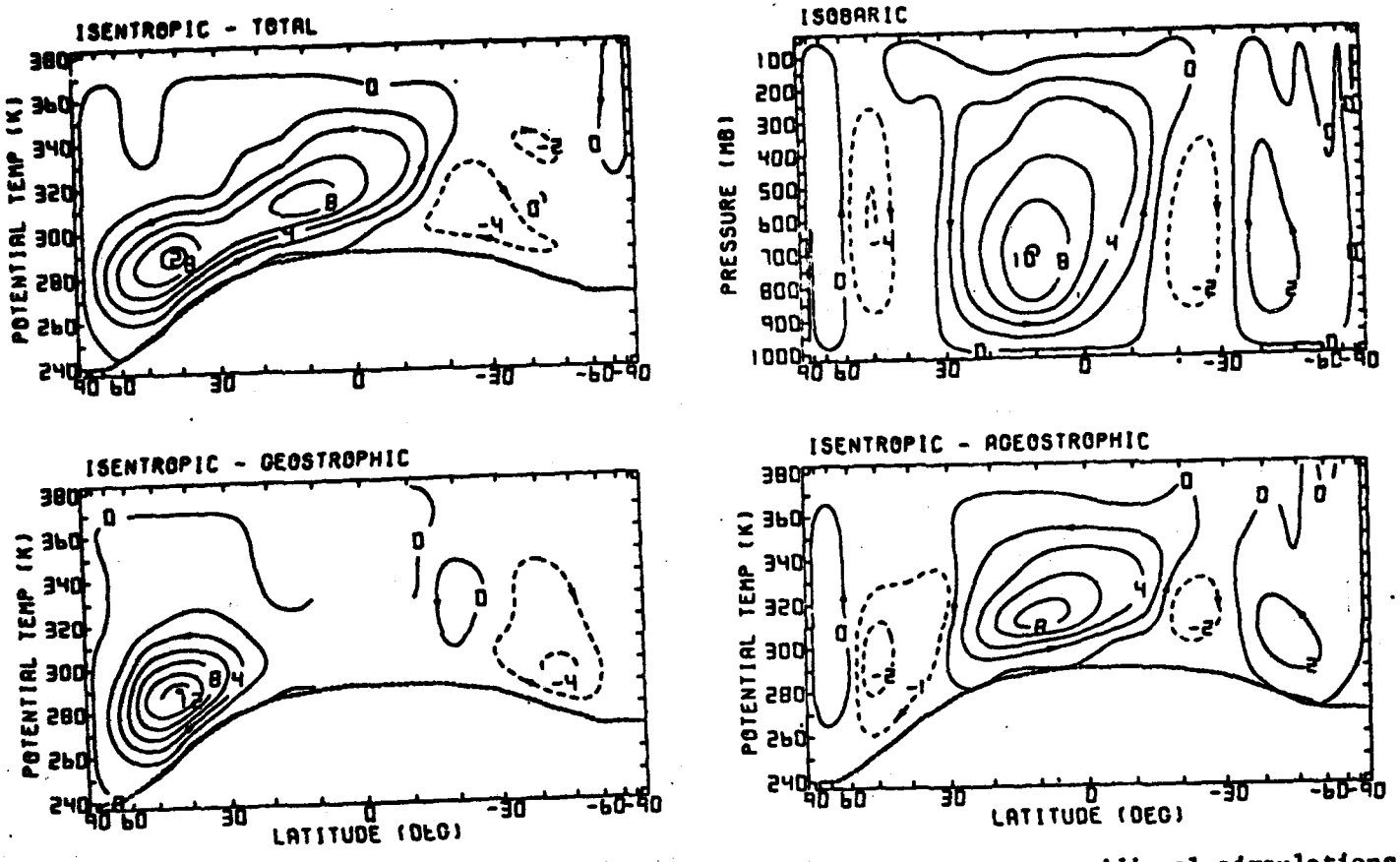

Figure 2. Mass stream function for the isobaric and isentropic mean meridional circulations for January 1979 (units, 10^{10} kg s^{-1}). Arrows indicate the direction of the circulation.

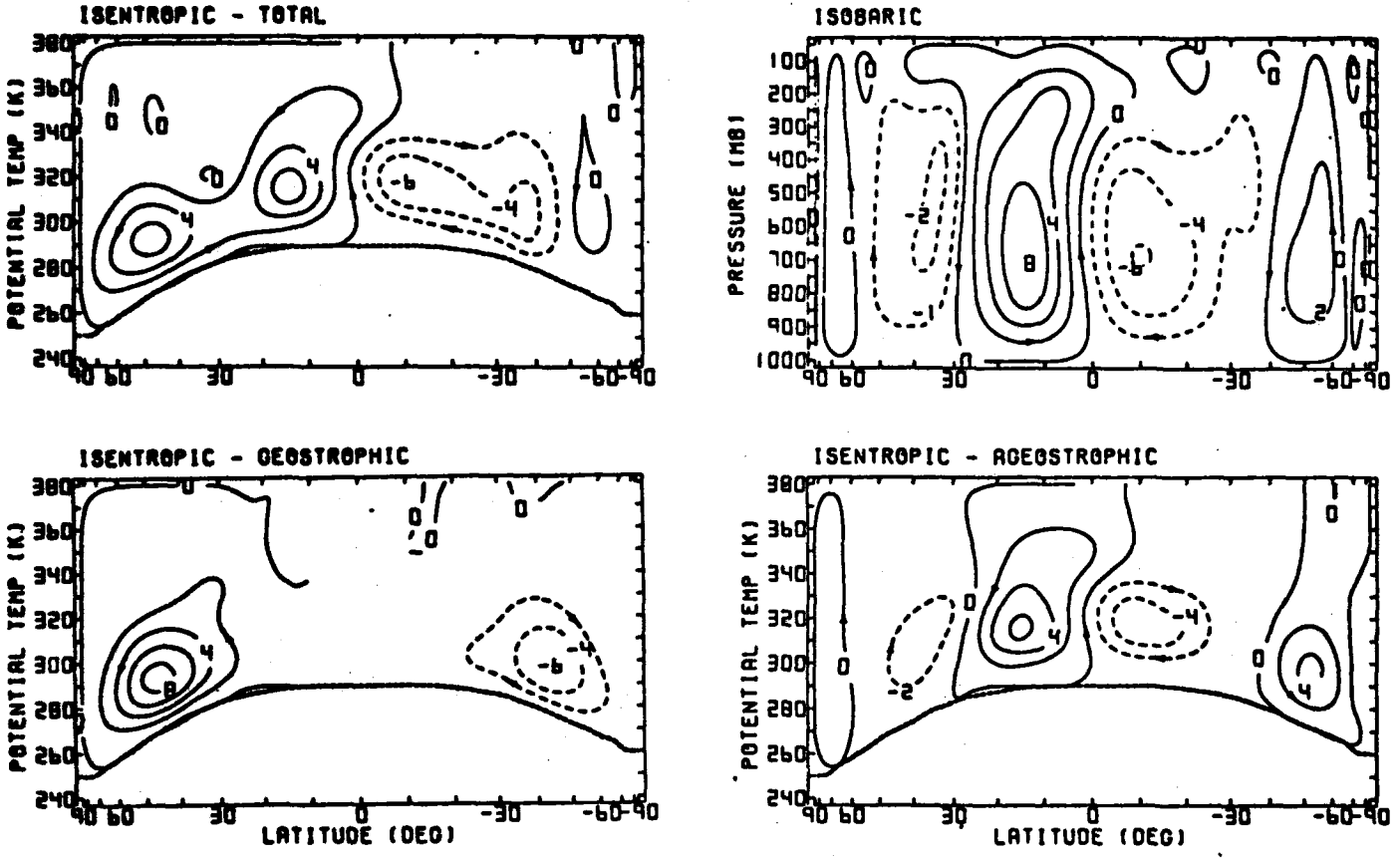

Figure 3. Mass stream function for the isobaric and isentropic mean meridional circulations for April 1979 (units, 10^{10} kg s^{-1}). Arrows indicate the direction of the circulation.

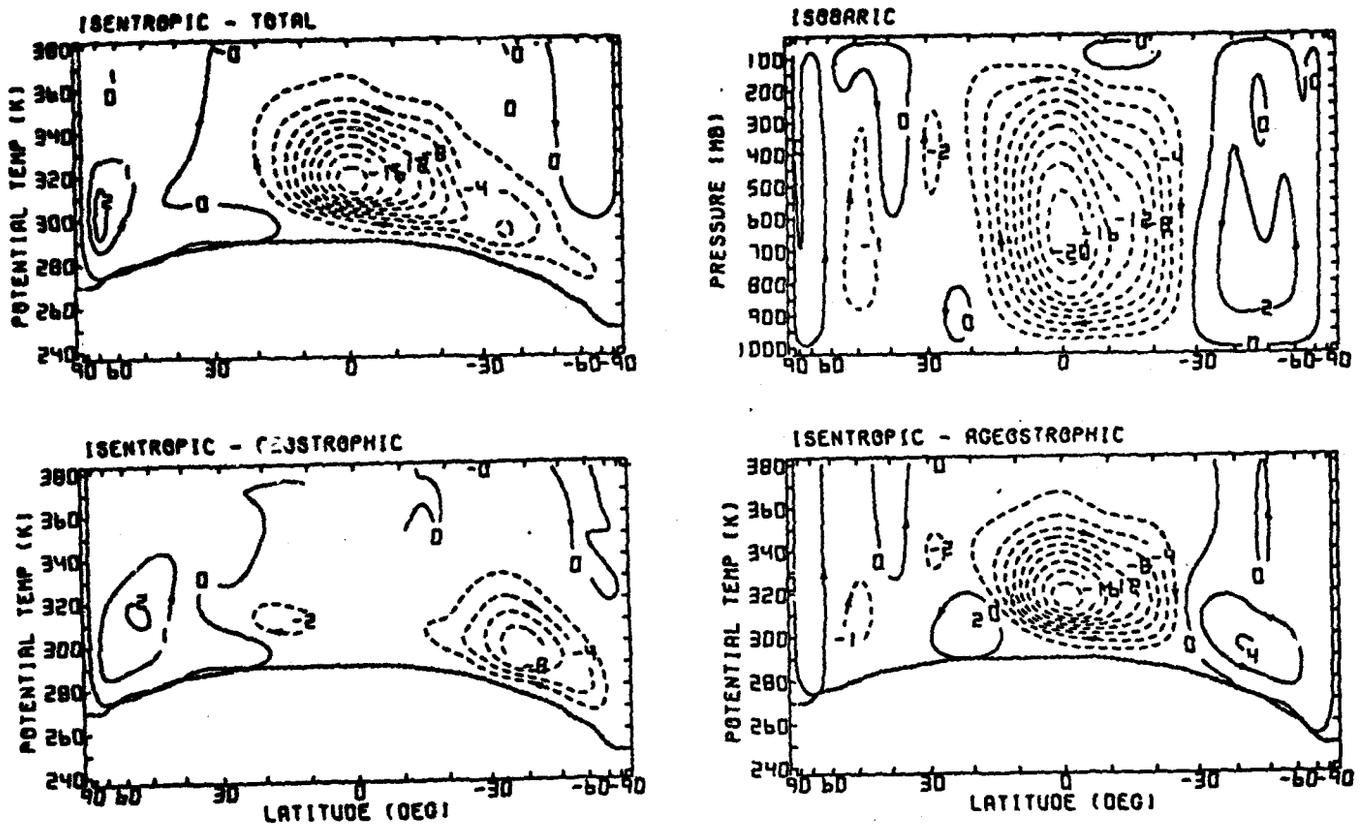

Figure 4. Mass stream function for the isobaric and isentropic mean meridional circulations for July 1979 (units, 10^{10} kg s^{-1}). Arrows indicate the direction of the circulation.

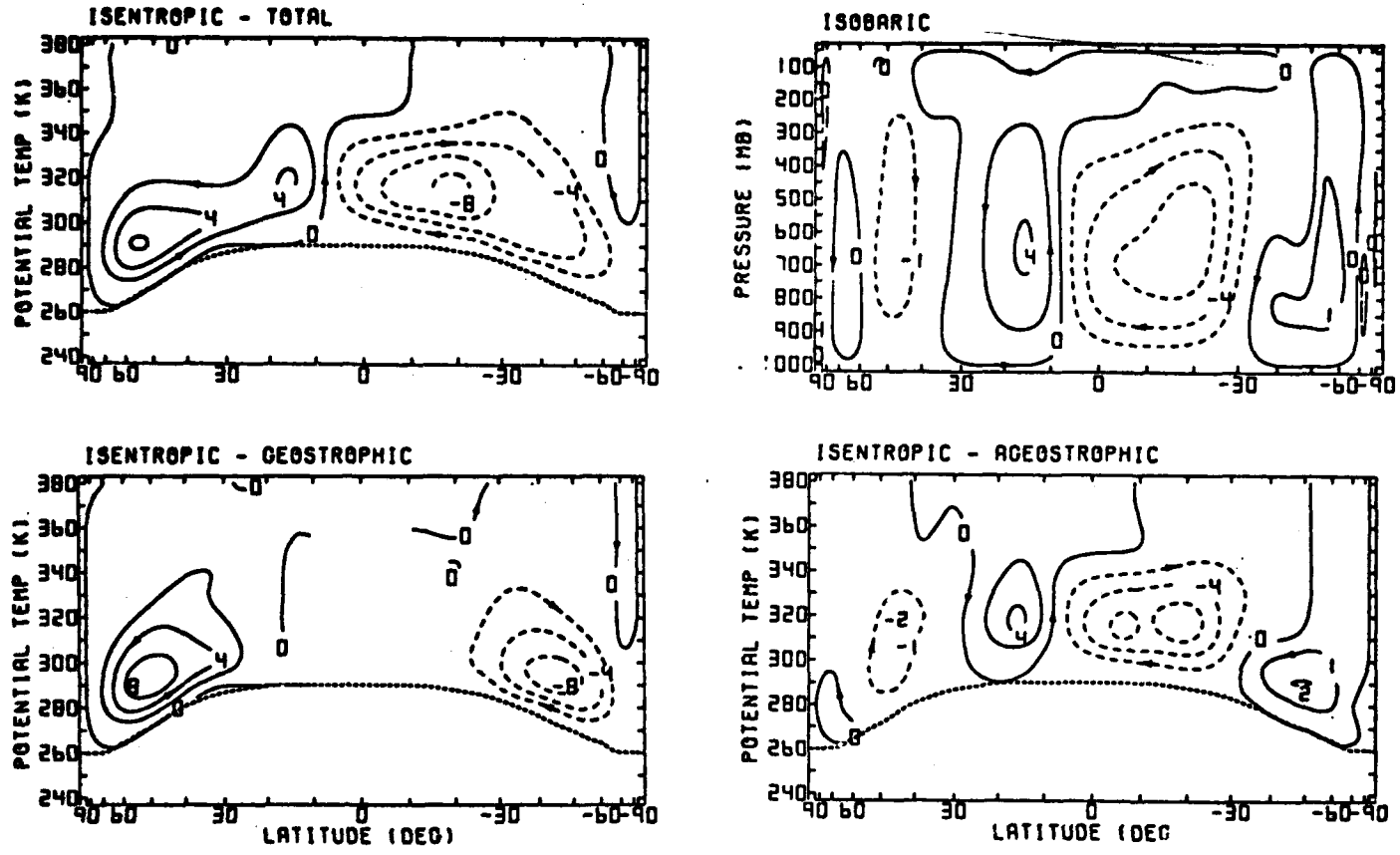

Figure 5. Mass stream function for the isobaric and isentropic mean meridional circulations for October 1979 (units, 10^{10} kg s^{-1}). Arrows indicate the direction of the circulation.

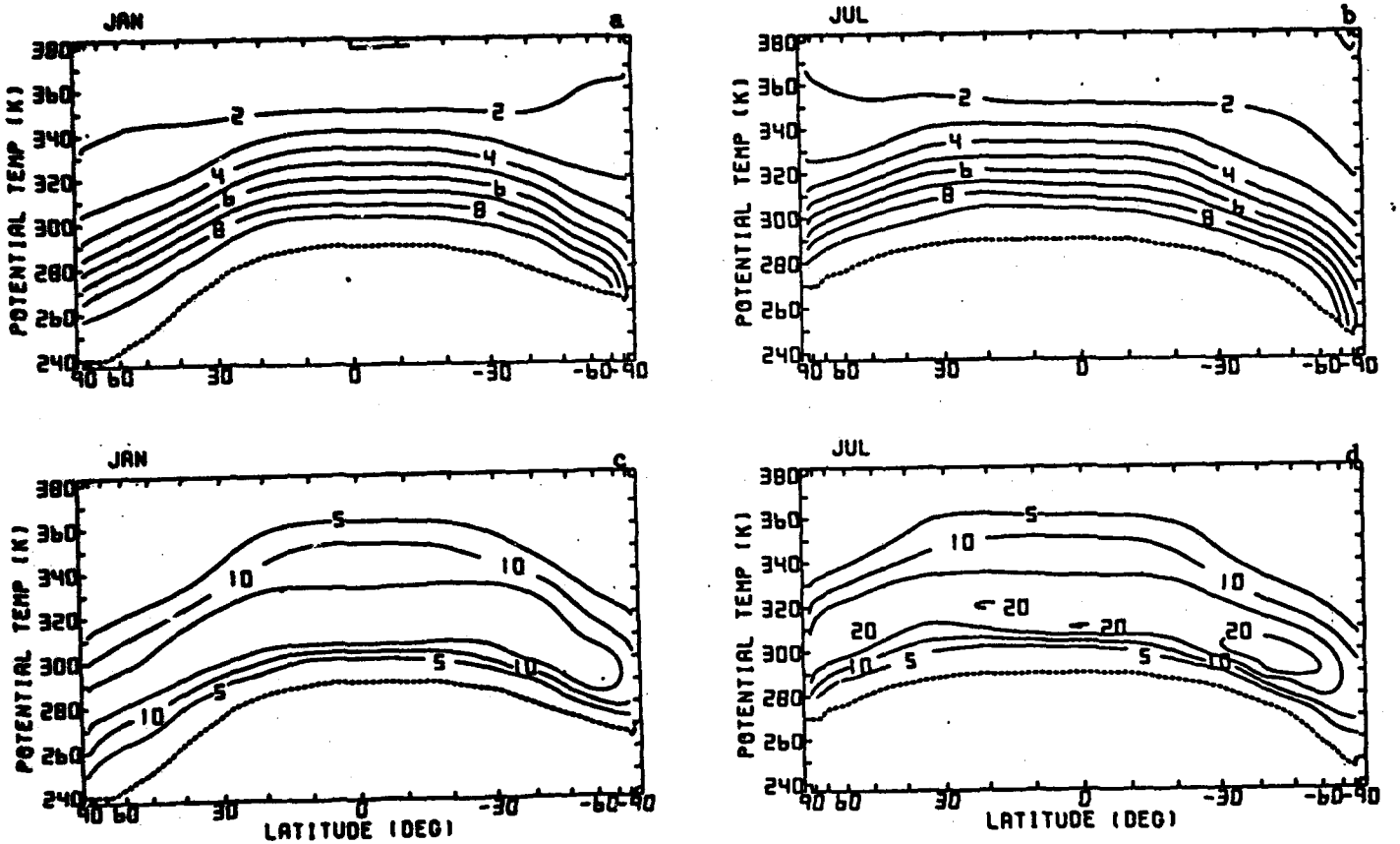

Figure 6. Meridional cross-sections of time and zonally-averaged pressure on an isentropic surface for January(a) and July(b) of 1979 (units, 10^2 mb) and time and zonally-averaged hydrostatic mass distribution ($\overline{\rho J_\theta}$) for January(c) and July(d) of 1979 (units, 10 kg m^2 K^{-1}).

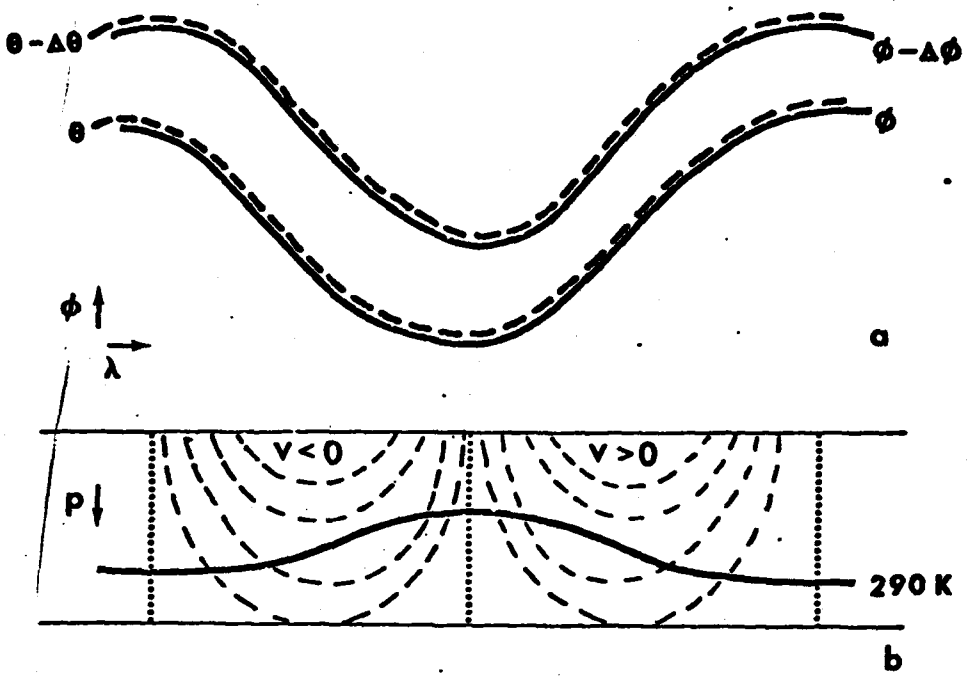

Figure 7. Schematics of horizontal (λ,ϕ) and vertical (λ,p) distributions of geopotential and potential temperature within a steady baroclinic wave. In the zonal, vertical cross-section the dashed lines designate trough and ridge positions which separate regions of poleward and equatorward geostrophic motion within two isentropic layers. The layer in 7b extends from a lower isentrope θ_ℓ to an intermediate isentrope θ_m to an upper isentrope θ_u (Figure after *Johnson*, 1979).

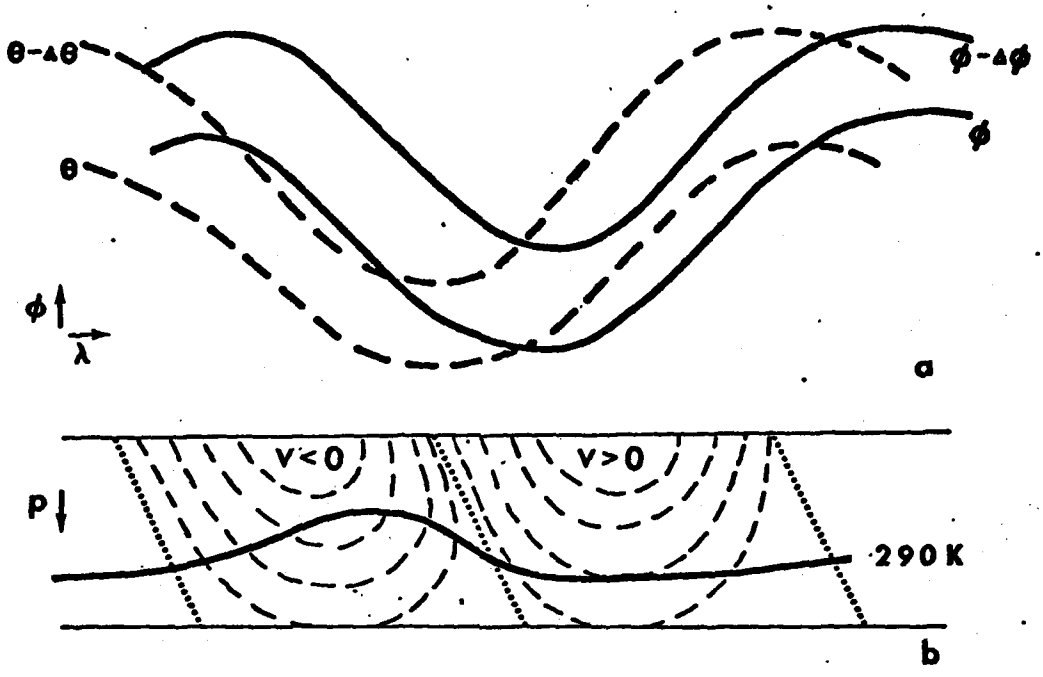

Figure 8. Schematic of amplifying baroclinic wave, see legend of Figure 7 for structural details (Figure after Johnson, 1979).

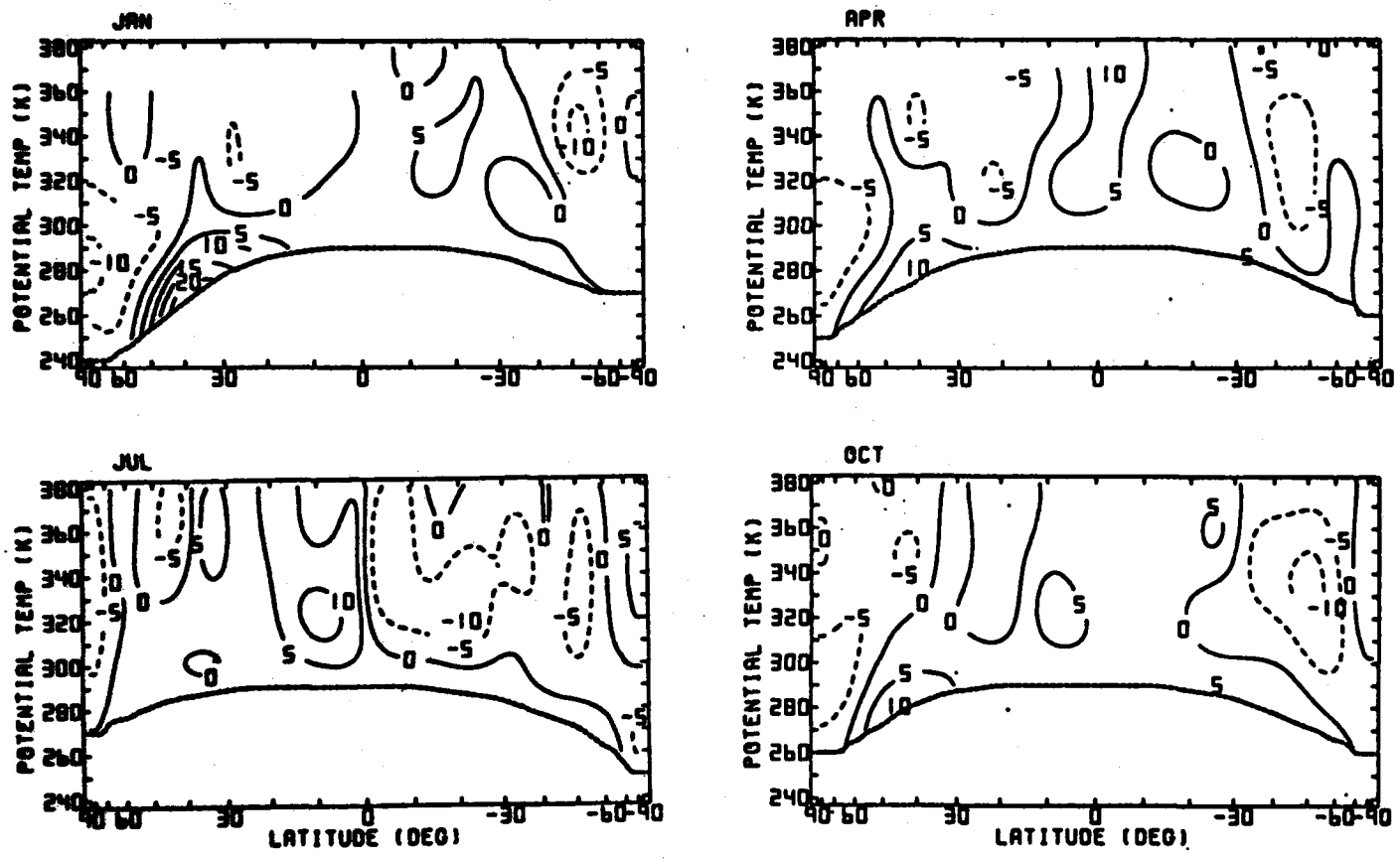

Figure 9. Meridional cross-sections of mass-weighted, time and zonally-averaged diabatic heating for January, April, July, and October 1979 (units, 10^{-1} K day^{-1}).

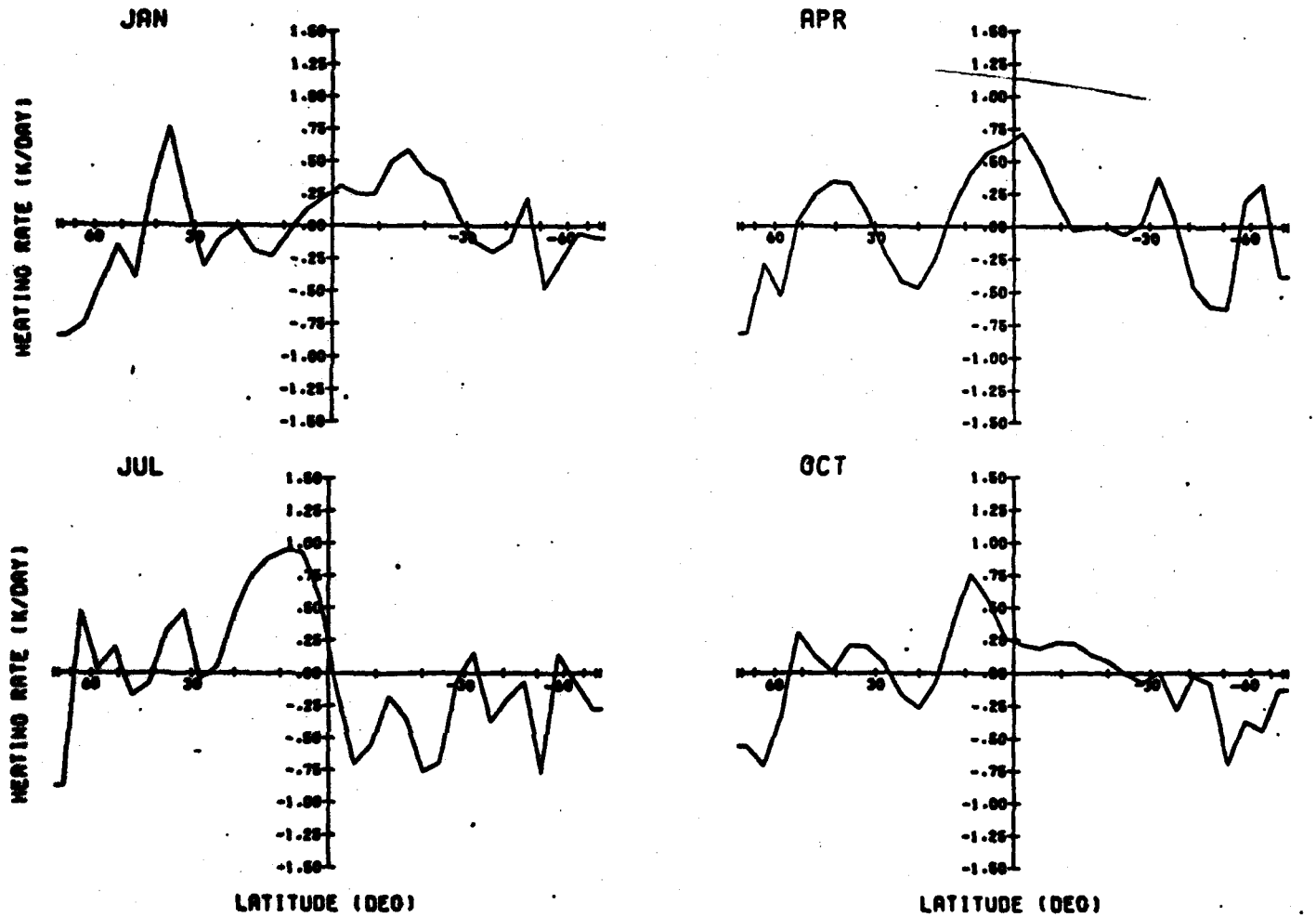

Figure 10. Mass-weighted vertical average of time and zonally-averaged diabatic heating for January, April, July, and October 1979 (units, K day^{-1}).

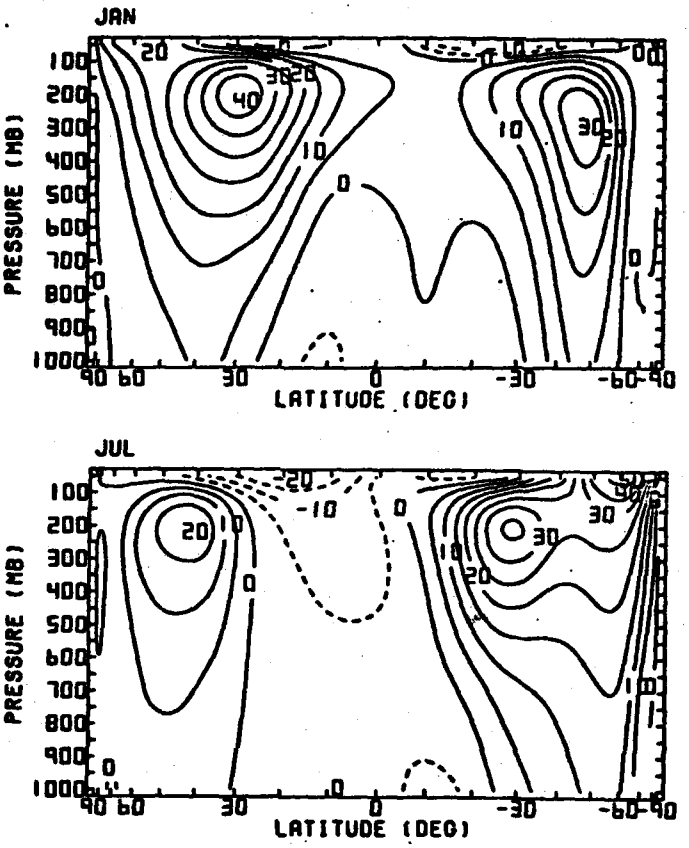

Figure 11. Meridional cross-sections of time and longitudinally-averaged zonal wind component ($\bar{u}$) in isobaric coordinates for January and July 1979 (units, m s^{-1}).

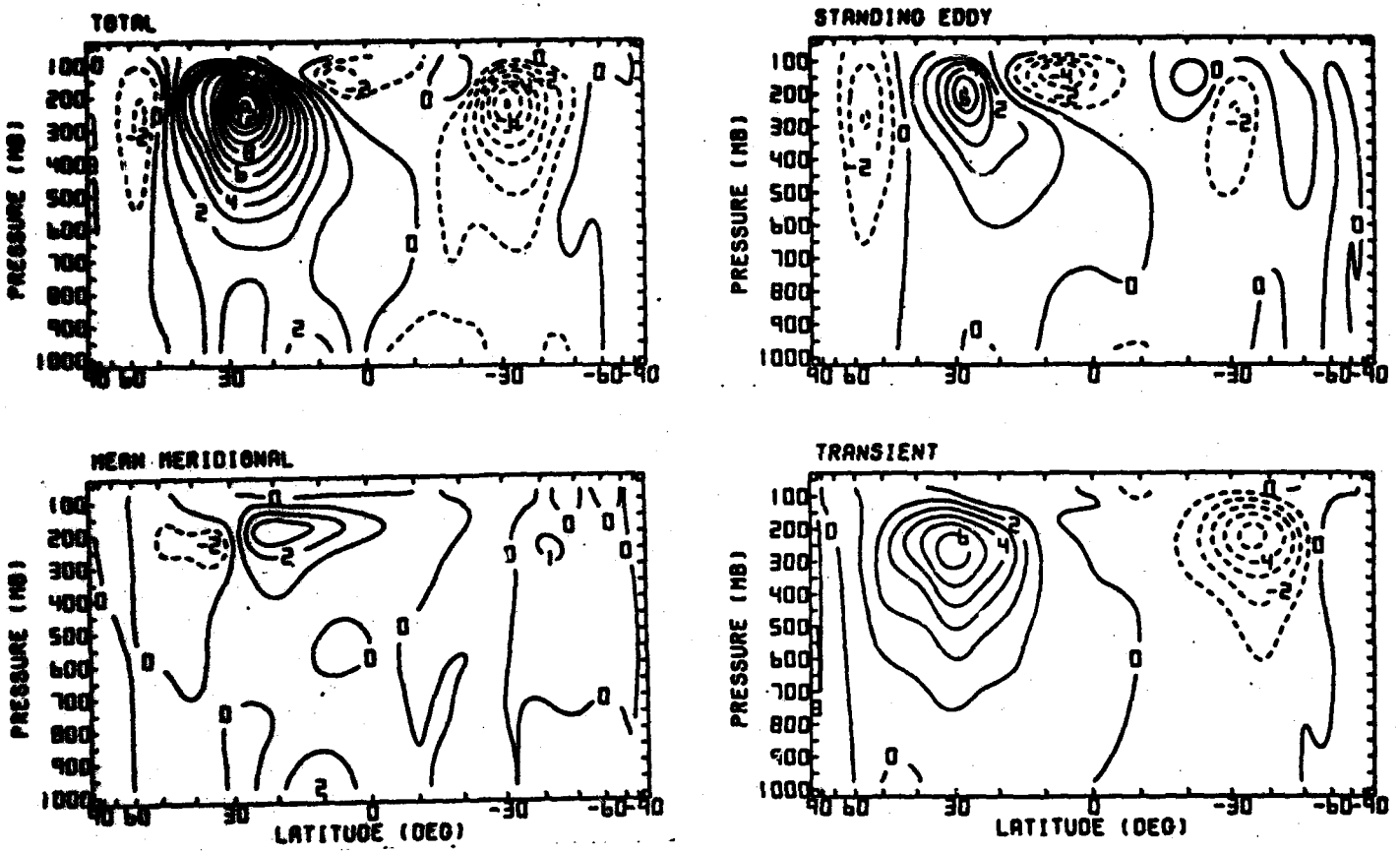

Figure 12. Meridional cross-sections of the total, mean meridional, standing eddy, and transient transport of relative angular momentum in isobaric coordinates for January 1979 (units, 10^{16} kg m^2 s^{-2} mb^{-1}).

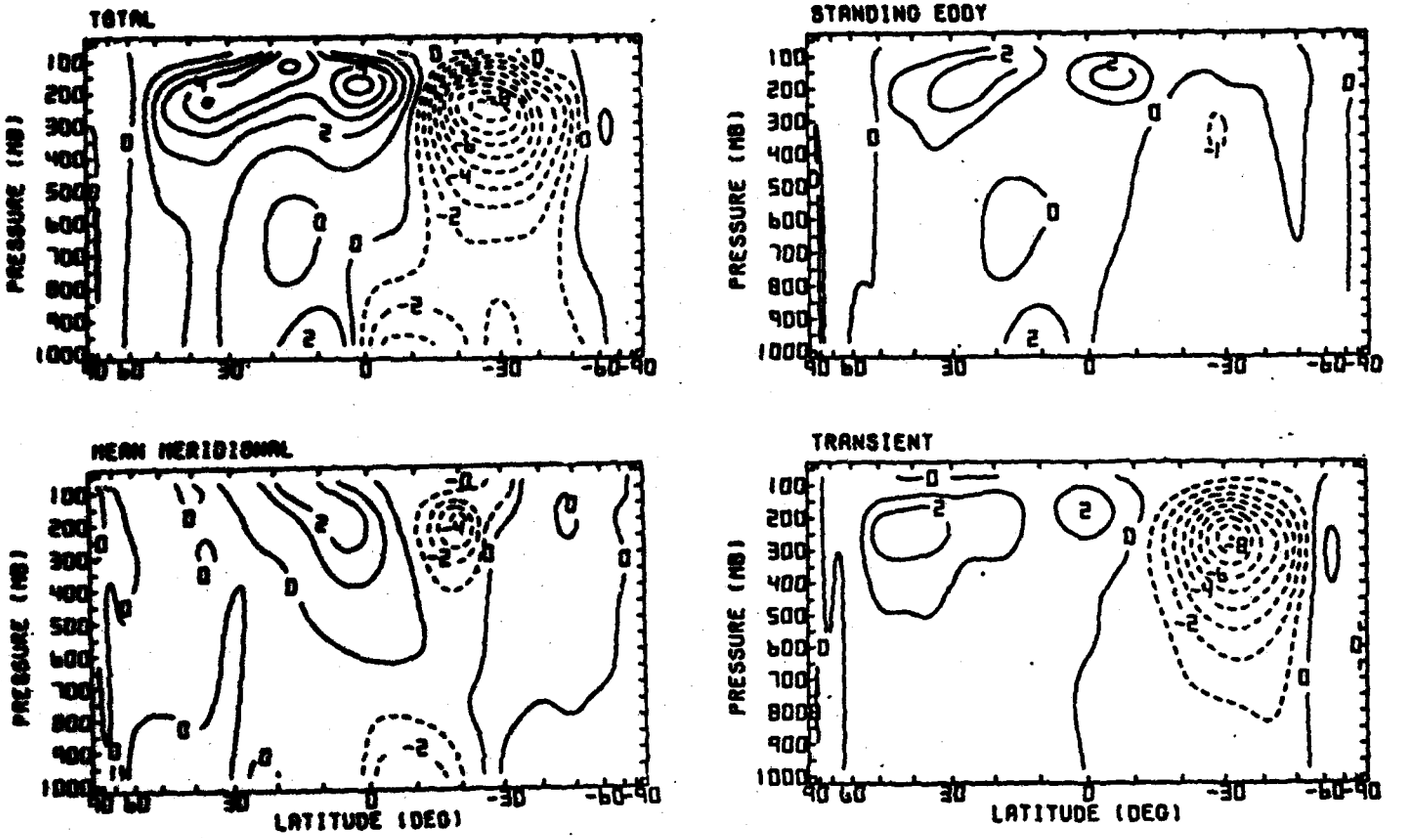

Figure 13. Meridional cross-sections of the total, mean meridional, standing eddy, and transient transport of relative angular momentum in isobaric coordinates for July 1979 (units, 10^{18} kg m^2 s^{-2} mb^{-1}).

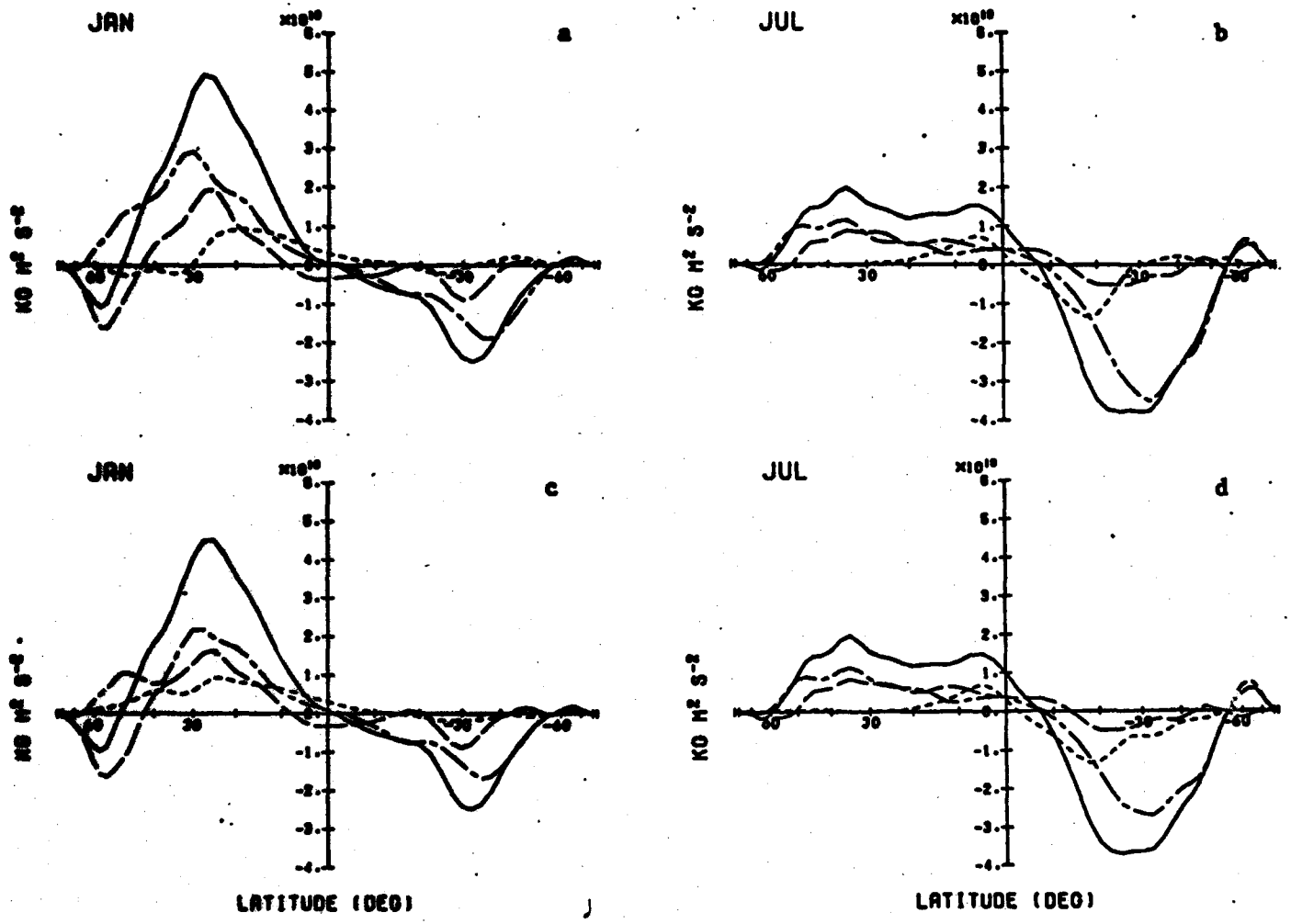

Figure 14. Meridional profiles of vertically integrated transport of total relative angular momentum and its component parts for January and July 1979 in isobaric coordinates(a and b) and isentropic coordinates(c and d) (units, 10^{19} kg m^2 s^{-2}).

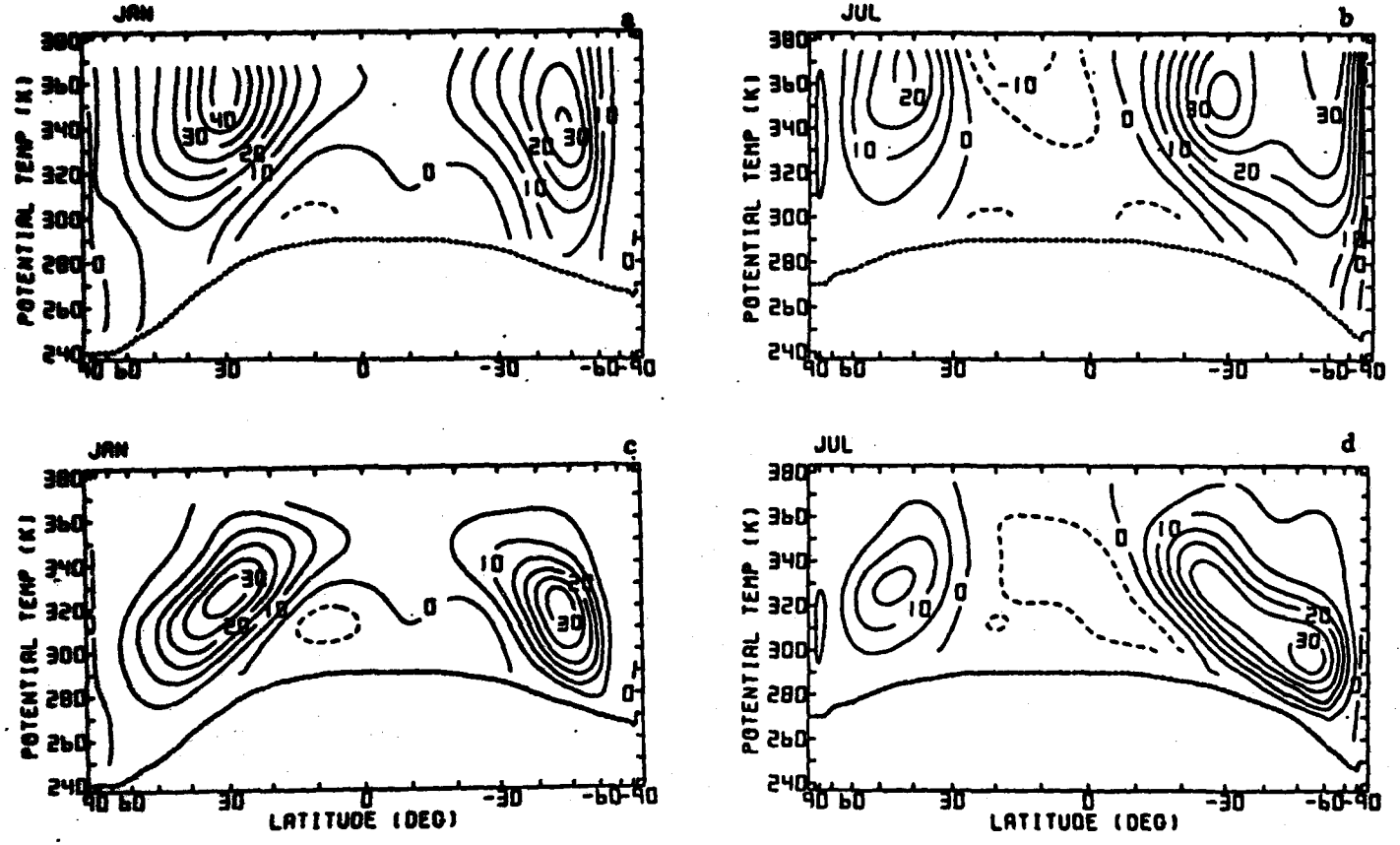

Figure 15. Meridional cross-sections of mass-weighted, time and longitudinally-averaged zonal wind component, $\bar{u}$; (a and b) in isentropic coordinates (units, m s^{-1}) and time and longitudinally-averaged momentum, $\overline{\rho J_\theta u}$, (c and d) in isentropic coordinates for January and July 1979 (units, 10^2 (kg m s^{-1}) $m^{-2}K^{-1}$).

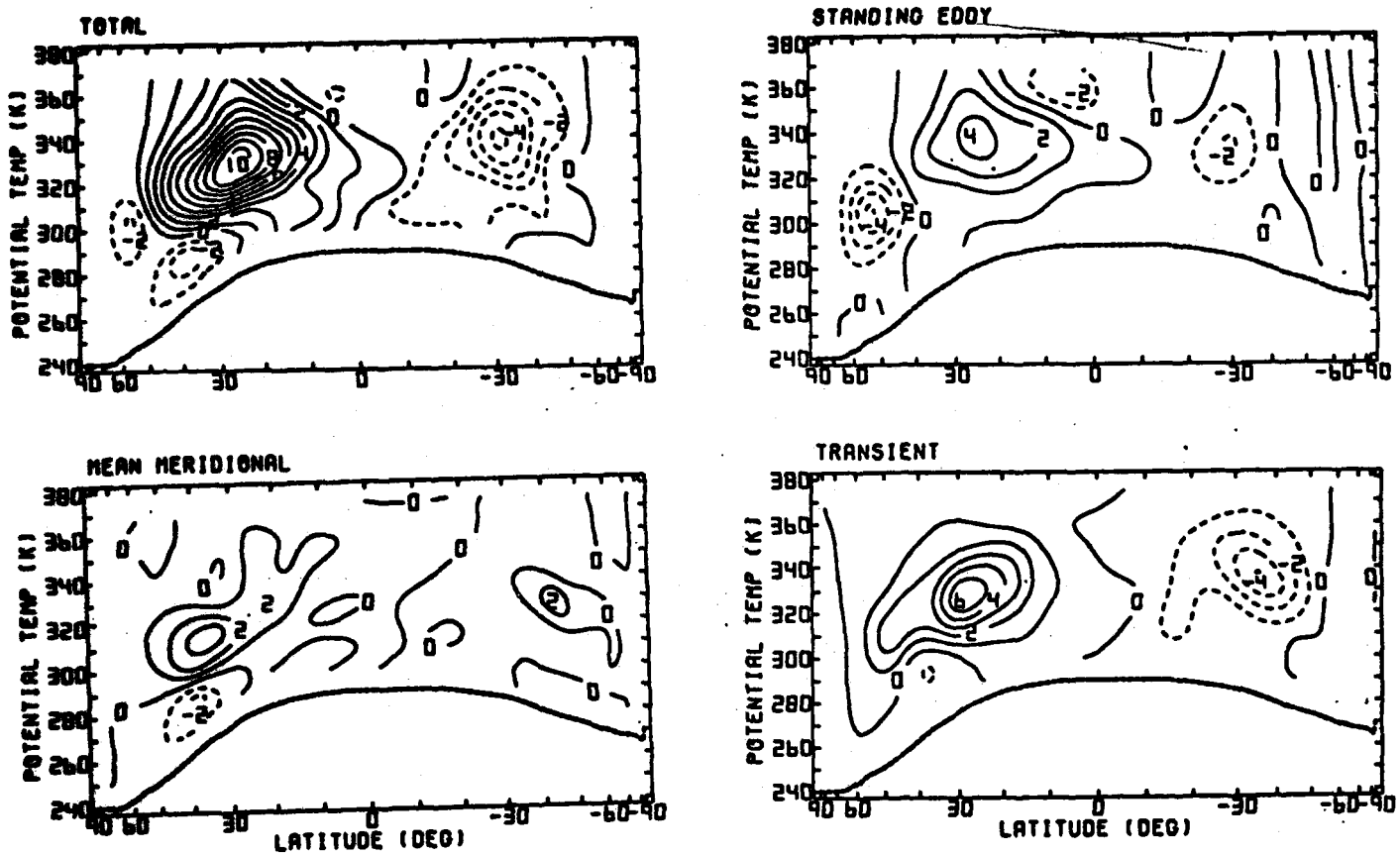

Figure 16. Meridional cross-sections of the total, mean meridional, standing eddy, and transient transport of relative angular momentum in isentropic coordinates for January 1979 (units, 10^{17} kg m^2 s^{-2} K^{-1}).

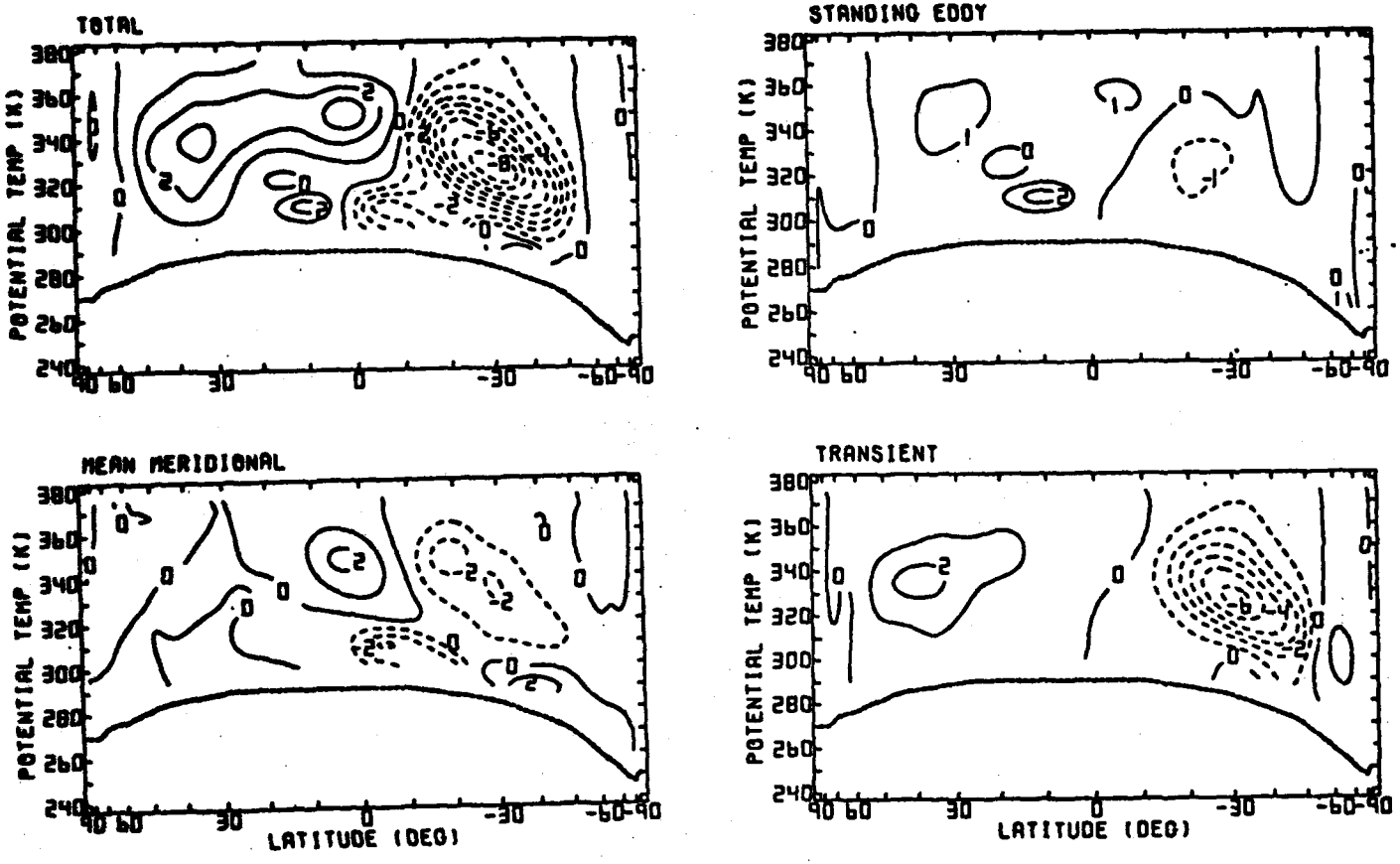

Figure 17. Meridional cross-sections of the total, mean meridional, standing eddy, and transient transport of relative angular momentum in isentropic coordinates for July 1979 (units, 10^{17} kg m^2 s^{-2} K^{-1}).